BMC Plant Biology

RESEARCH

Open Access

Genomic signatures of *SnRK*s highlighted conserved evolution within orchids and stress responses through ABA signaling in the *Cymbidium ensifolium*

Ruiyue Zheng[1†], Kai Zhao[2†], Jiemin Chen[1], Xuanyi Zhu[1], Yukun Peng[1], Mingli Shen[2], Zhong-Jian Liu[1], Donghui Peng[1] and Yuzhen Zhou[1*]

Abstract

Sucrose non-fermenting 1-related protein kinases (SnRKs) are crucial for modulating plant responses to abiotic stresses, linking metabolism with stress signaling pathways. Investigating the roles and stress responses of *SnRKs* in plants paves the way for developing stress-tolerant strategies in orchid species. Here, 362 *SnRK* members were identified from nine current orchid genomes, highlighting the conservation of these genes in evolution. Among these, 33 *CeSnRKs* were found across 20 chromosomes of *C. ensifolium* genome. Multiple duplication events increased the complexity of *CeSnRKs* during independent evolution. Moreover, distinct functional domains beyond the kinase domain differentiated the subfamilies. These multi-copy members existed tissue specific expressions falling into 6 main trends, especially *CeSnRK1*, *CeCIPK9*, *CeCIPK23* displayed a strict floral expression. ABA-related elements were enriched in the promoters of *CeSnRKs*, and stress-related miRNA binding sites were identified on partial *CeSnRK*s. Consequently, most *CeSnRKs* exhibited up-regulated expression during ABA treatment. Several genes, such as *CeSnRK2.1* and *CeCIPK28* involved growth and development at different times and various tissues. The up-regulation of *SnRK2.1*, along with high expression of *SnRK1* and *CIPK27* under drought stress, and the differential expression patterns of *CeSnRKs* under cold stress, underscore the involvement of *CeSnRK* genes in different stress responses. Additionally, the diverse interactions of CeSnRKs with proteins highlighted a multifaceted functional network.These findings offer valuable insights for the future functional characterization formation of *CeSnRK*s and the adaptive evolution of genes in orchids.

Keywords Evolution, Orchidaceae, Expression patterns, ABA response, Abiotic stress

†Ruiyue Zheng and Kai Zhao contributed equally to this work.

*Correspondence:
Yuzhen Zhou
zhouyuzhencn@fafu.edu.cn
[1]Ornamental Plant Germplasm Resources Innovation & Engineering Application Research Center, Key Laboratory of National Forestry and Grassland Administration for Orchid Conservation and Utilization, College of Landscape Architecture and Art, The Cross-Strait Scientific and Technological Innovation Hub of Flower Industry, Fujian Agriculture and Forestry University, Fuzhou 350002, China
[2]College of Life Sciences, Fujian Normal University, Fuzhou 350117, China

Introduction

Due to their sessile nature, plants are inherently vulnerable to abiotic stresses such as drought, heat, low temperatures, heavy metals, and salinity [1]. Consequently, these stresses disrupt various physiological processes, including the plant biological clock, metabolic substance synthesis, and signal transmission [2–4]. Despite China's vast territory and abundant resources, environmental challenges remain formidable [5, 6]. Issues like soil salinization in northwest China, recurrent nationwide droughts, and the expansion of regions subjected to extreme high temperatures significantly impede plant growth and development [7–9]. Hence, numerous scholars are dedicated to investigating the responses of plants to various stressors in order to explore strategies for mitigating the environmental challenges encountered by plants. For instance, researchers has focused on the physiological responses of different asparagus cultivars, peanut, and quinoa to salt stress [10]. *CtFLS1* from safflower has been found to mitigate drought stress. and the *WRKY* gene in tea plant exhibits responses to diverse stressors [11]. *Cymbidium ensifolium*, cultivated in Fujian Province, China, boasts remarkable ornamental and economic significance [12, 13]. With the continual progress in the orchid industry, a diverse array of horticultural orchid varieties has been developed [14, 15]. Presently, *C. ensifolium* serves as a crucial economic asset distributed nationwide. However, their persistence in the wild, introduction, and cultivation face numerous challenges attributed to abiotic stressors. As a economic orchid, *C. ensifolium*, is often used as a typical material for orchid researches. Hence, delving into the response of *C. ensifolium* to abiotic stress promises substantial contributions to the realms of orchid breeding, cultivation, and the development of the orchid industry.

Plants exhibit adaptive responses to diverse abiotic stresses through the modulation of gene expression and protein modifications, including kinase-mediated phosphorylation [16, 17]. Among the crucial players, SnRK, a serine/ threonine protein kinase, orchestrates various physiological activities in plants [18]. Phylogenetic analysis delineates the *SnRK* family into three distinct subfamilies: SnRK1, SnRK2, and SnRK3 [19]. The SnRK family comprises three essential domains: the kinase domain, UBA domain, and KA1 domain, each exhibiting distinctive functionalities. While the UBA domain is associated with ubiquitination, the KA1 domain intricately interacts with phosphatases [20–22]. Notably, the SnRK1 subfamily stands out for its highly conserved N-terminal catalytic domain [23]. Members of the SnRK2 subfamily share a common N-terminal kinase domain and have additional domains at the C-terminus, including domain I and ATP-binding domains [24]. SnRK3, alias Calcineurin B-like protein-interacting protein kinases (CIPK), interacts intricately with calcineurin B-like protein (CBL), thereby regulating calcium signaling in plants. Besides kinase domain, they exhibit two conserved domains at their C-terminus: NAF and PPI [25, 26].

The *SnRK* gene family in plants plays pivotal roles in metabolic regulation, plant growth and development, and responses to abiotic stress. SnRK1 functions as a central signaling hub governing plant growth and development. It modulates the E2Fa protein to regulate growth in *Arabidopsis thaliana* [27, 28]. Furthermore, during sugar deprivation, *OsSnRK1a* interacts with *OsSGI1*, thereby augmenting the transcriptional repression of *OsTPP7*, consequently perturbing sugar homeostasis and impeding rice growth [29]. Conversely, *SKINs* exert antagonistic effects with *SnRK1A* under various stress conditions, such as drought, thereby modulating seedling growth [30]. In *Dendrobium officinale*, the expression of *DoSnRK1.1* diminishes under drought, JA, and abscisic acid (ABA) stress [31]. The *SnRK2* gene is pivotal in orchestrating plant growth and mediating environmental responses [32]. Under salt stress conditions, both SnRK2 protein and mRNA decapping machinery influence on *Arabidopsis* root development [33]. Moreover, *Arabidopsis PCaP2* triggers the activation of the *CBF* and SnRK2-mediated transcriptional regulatory network to bolster cold tolerance [34]. Fundamental regulatory pathways in plants' response to ABA involve *PYL*, *PP2C*, and *SnRK2* [35]. The *CePP2C19* enhances drought tolerance of *Cyperus esculentus* by reducing ABA sensitivity [36]. Ubiquitin-mediated negative regulation of ABA response hinders the activities of SnRK2.2 and SnRK2.3 kinases in *Arabidopsis* [37]. Meanwhile, the SnRK2.6 kinase activates ABA signaling by modulating MAPKKK18 [38]. The SnRK3 subfamily, termed the CIPK subfamily, encompasses kinases intricately linked with calcium ion channels [39]. CIPK engages with calcineurin B-like protein to elicit responses to diverse stimuli or stress signals. In rice, it experiences significant induction in response to cues such as cold, light, and salt [40, 41]. In *Arabidopsis*, the calcium signaling pathway under salt stress is sensed by *SOS3* (*AtCBL4*), which forms a complex with *SOS2* (*AtCIPK24*) to phosphorylate *SOS1*, thereby facilitating the removal of Na^+ from root cells [42, 43].

Consequently, the plant *SnRK* family assumes a crucial role in responding to abiotic stressors and metabolism-related tissue development. With the advancement of research into the plant *SnRKs*, *SnRK* genes have been identified across diverse species, including *Casuarina equisetifolia* [42], *Liriodendron chinense* [22], *Rubus occidentalis* [44] and *D. officinale* [31], among others. The orchid industry is rapidly developing with high economic benefits, exerting a significant role in promoting economic development [15]. But, its progress is hindered by various environmental issues [45, 46]. As a

result, researchers are focusing on the stress resistance of orchids, which involves several related gene families, such as *AREB/ABF* [47], *NF-Y* [48], and *HSF* [49]. The *SnRK* gene family is pivotal in investigating plant responses to abiotic stress, making it essential for exploring the stress resistance of orchids. Nonetheless, there is a notable lack of studies on the *SnRK* gene family in orchids. Many orchids possess high economic value, such as *Phalaenopsis*, *Dendrobium*, *Anoectochilus*, and *Cymbidium* [50]. *C. ensifolium*, an important orchid within the *Cymbidium* genus, is widely cultivated due to its unique color, leaf pattern and fragrance, and has emerged as an indispensable economic orchid [13]. The extensive variety, growing areas and disease resistance characteristics of *C. ensifolium* also makes it a typical material for orchid research [13, 51–53]. Thus, using *C. ensifolium* as the primary research subject to explore its response mechanisms to abiotic stress is a compelling topic. Such investigations bear significant implications for the improvement of breeding techniques, cultivation practices, and the overall advancement of the orchid industry.

This study comprehensively identified the *SnRK* genes in the current orchid genomes and taking *C. ensifolium* as an example, the specific gene expression structures and profiles were analyzed. Through analysis of phylogeny, gene structure, cis-elements, protein interaction network, miRNA binding sites, phosphorylation sites, and gene expression patterns, we obtained the basic transcriptional regulatory structure, and thus underpinning the utilization and improvement of *CeSnRKs*. These findings represented a foundational step towards unraveling the intricate molecular mechanisms underlying the resilience of *C. ensifolium* to abiotic stress. They also provide a solid background for detecting natural metabolic formation and further genome editing for genetic improvement.

Results

Identification and phylogenetic analysis of *SnRK* genes in Orchidaceae genomes

Based on the reference sequence of *A. thaliana* SnRK proteins, an investigation of the *SnRK* gene family in various species of Orchidaceae was conducted throughout our local database. A total of 362 *SnRK* genes were identified across nine species of Orchidaceae, 51 were found in *D. catenatum*, 33 in *D. chrysotoxum*, 37 in *D. nobile*, 38 in *G. elata*, 35 in *P. aphrodite*, 64 in *P. equestris*, 30 in *A. shenzhenica*, 41 in *V. planifolia* and 33 *C. ensifolium* (Fig. 1 and Supplementary File S1). To understand the homologous relationships of *SnRK* genes among diverse orchids, we performed a direct identification analysis of orthologous genes in these orchids. From the 362 *SnRK* genes identified in nine orchid species, we found 2354 orthologous pairs and 22 groups (Supplementary Table S1A and 1B). Orthologous pairs were present in each orchid, with quantities varying among species. Among the 22 orthologous groups, the nine orchids with *SnRK* genes clustered into groups 1, 4, 5, 9, and 18, with group 1 containing the most genes. Additionally, no chimeric proteins were identified. Among the above nine orchids, *D. catenatum*, *D. nobile* and *D. chrysotoxum* are epiphytic or lithophytic, *P. equestris*, *V. planifolia* and *P. aphrodite* are epiphytic; *C. ensifolium* and *A. shenzhenica* are terrestrial; and *G. elata* is fully mycoheterotrophic. According to previous phylogenetic studies, orchids with different life forms exhibited different evolutionary positions. Some terrestrial orchids, such as *V. planifolia* and *A. shenzhenica*, may have diverged first, followed by fully mycoheterotrophic orchids. Subsequently, epiphytic and lithophytic orchids diverged. Distinct evolutionary positions among the nine orchids, with varying numbers of *SnRK* genes (Fig. 1A and C). Most species of Orchidaceae in this study exhibited a relatively consistent range of *SnRK* gene numbers, typically between 30 and 41. All orchids exhibited three subfamilies of *SnRK* genes. SnRK3 consistently represented the most abundant subfamily across all species, while SnRK1 consistently exhibited the least abundance. The earliest to diverge, *A. shenzhenica* and *V. planifolia*, possessed 30 and 41 members, respectively. In contrast, The later diverging orchids, *D. catenatum* (51) and *P. equestris* (64), exhibited a higher number of *SnRK* genes compared to other orchids. Overall, the number of *SnRK* genes varied among orchids situated at different evolutionary positions.

However, *C. ensifolium*, another terrestrial orchid, was the last to diverge. (Fig. 1A). A phylogenetic tree was constructed combining these SnRK proteins. The results revealed that CeSnRK proteins were classified into three evolutionary branches: SnRK 1, SnRK 2, and SnRK 3 subgroups (Fig. 1B). In *C. ensifolium*, the SnRK1 subgroup had the fewest members with only one, while the SnRK3 subgroup had the most members with 28. Following the chromosome positions of *C. ensifolium SnRKs* and adhering to *Arabidopsis* nomenclature conventions, *CeSnRKs* were named as *CeSnRK1*, *CeSnRK2.1-CeSnRK2.4*, and *CeCIPK1-CeCIPK28* (Supplementary Table S2). Analysis of various physicochemical properties of CeSnRK proteins revealed lengths ranging from 350 to 509 amino acids, molecular weights from 40,434.92 to 57,925.26 Da, theoretical isoelectric points from 4.89 to 9.44, instability indices from 29.45 to 60.15, aliphatic indices from 77.96 to 98.59, and grand average of hydropathicity from – 0.655 to – 0.131 (Supplementary Table S2).

Gene structure and composition of *CeSnRK*s

According to the multiple sequence alignment results of protein sequences, CeSnRKs exhibited conserved domains (Fig. 8). The serine/threonine protein kinases

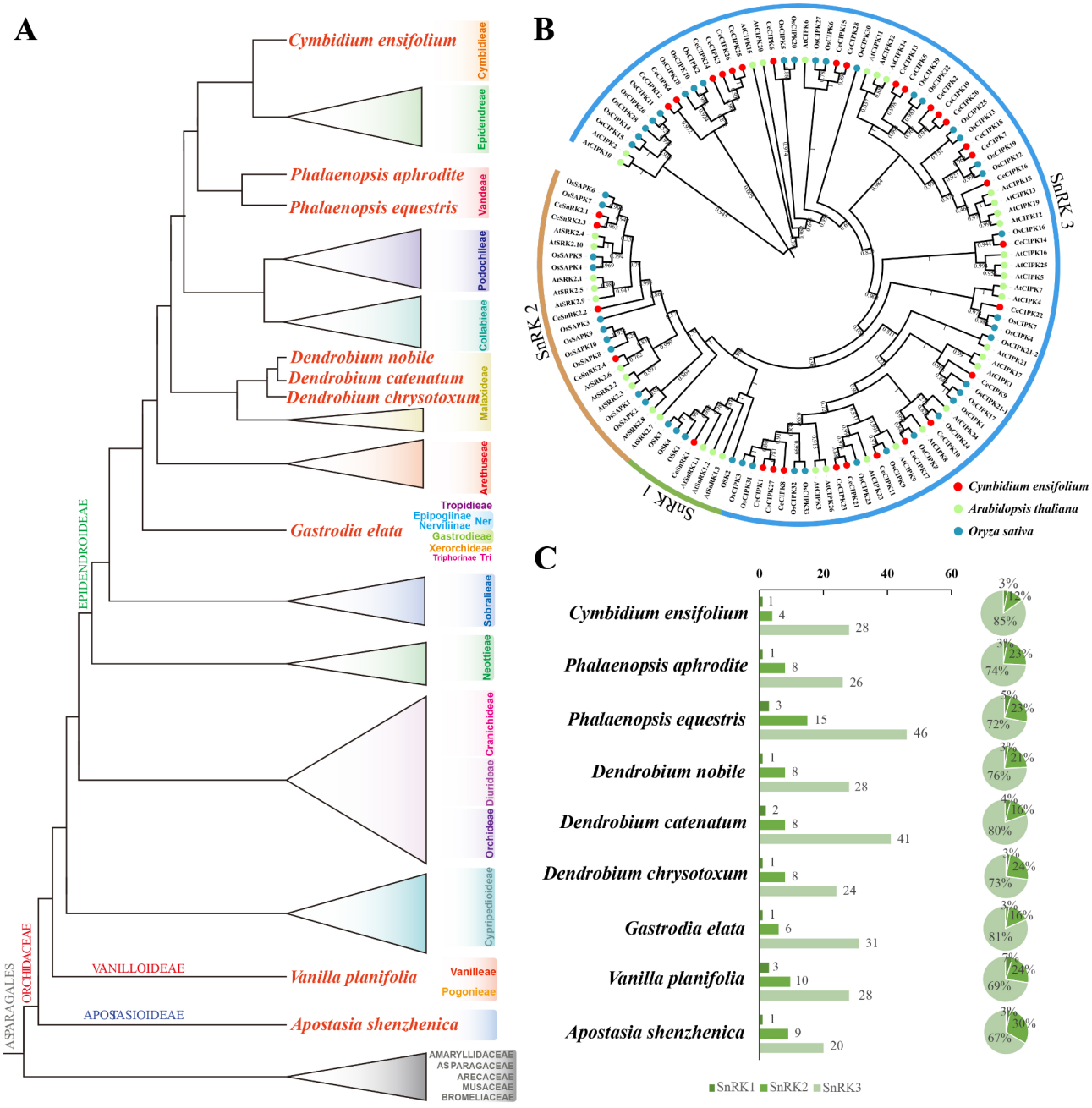

Fig. 1 Phylogenetic analysis and *SnRKs* statistics of different orchids. **(A)** Phylogenetic analysis of Orchidaceae from previous study [57]. **(B)** Phylogenetic tree of *SnRK* genes in three plant species. The neighbor-joining (NJ) phylogenetic tree was constructed using PhyloSuite with 1000 bootstraps. **(C)** Statistical analysis of *SnRK* genes in different orchid species

active site were identified in CeSnRK2 members, along with other domains including the ATP binding site and Domain I. Highly conserved kinase domains were found in all CeSnRK3 members, along with the NAF and PPI domains were located at the C-terminus. For a deeper understanding of genetic evolution and gene structure, the gene structures of 33 *CeSnRKs* were analyzed, including conserved motifs, exons, introns, CDS, and UTRs (Fig. 2). Motif analysis revealed that all CeSnRK proteins contain motifs 4, 2, 7, 1, and 5, while motif 3 were present in all CeSnRK members except for CeCIPK26 (Fig. 2A and C). Besides the similarity in motifs among all CeSnRK members, motifs within the same subfamily also exhibited certain regularities. Motif 15 was found exclusively in the CeSnRK2 subfamily, while motifs 13, 9, 10, 6, 12, and 14 were only present in the CeSnRK3 subfamily. The differential conservation of motifs among different subfamilies emphasizes the conservation of genetic

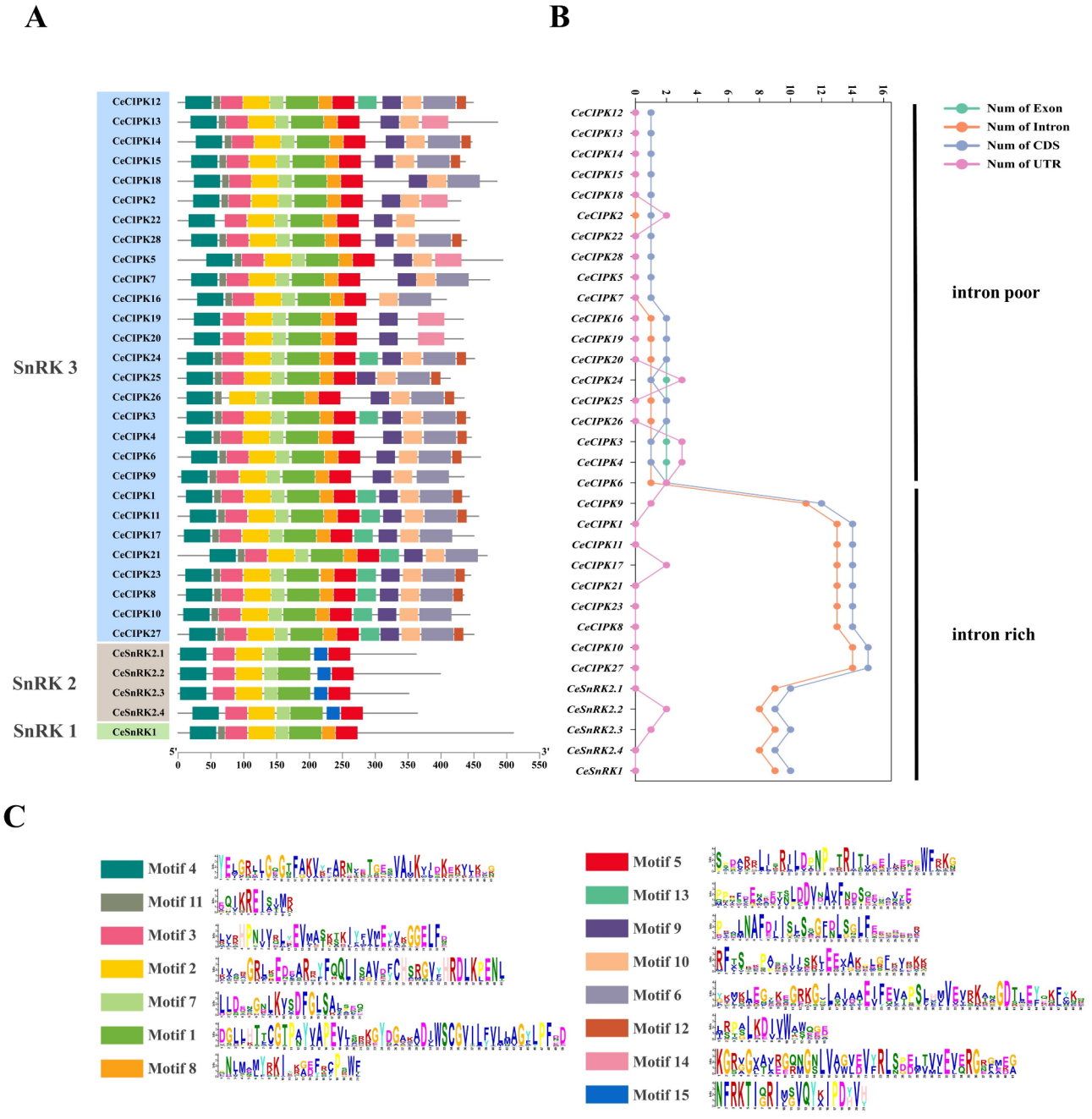

Fig. 2 Gene structures and conserved motif analysis in *Cymbidium ensifolium SnRKs*. **(A)** The conserved motifs of *Cymbidium ensifolium* SnRK proteins. **(B)** Gene structure statistics of *CeSnRKs*, including introns, exons, CDSs, and UTRs. **(C)** Detailed presentation of conserved motifs in CeSnRK proteins

structure and function. In the analysis of exons, introns, CDS, and UTRs, notable differences in intron numbers among *CeSnRKs* were observed (Fig. 2B), classifying them into two categories: intron poor and intron rich. Members of the CeSnRK1 and CeSnRK2 subfamilies contain a higher number of introns, while 67.9% (19/28) of members in the CeSnRK3 subfamily had a low number of introns (0 or 1). *CeCIPK10* and *CeCIPK27* exhibited the highest number of introns, with 14 each, highlighting the diversity of gene functions. Analysis also indicated that changes in exon/ CDS numbers parallel those of introns, while UTR numbers range from 0 to 3.

Tertiary structures of the CeSnRK proteins

The functionality of proteins is closely associated with their structure. Therefore, the secondary structure of CeSnRK proteins was predicted using the CFSSP database. The results revealed that the secondary structure mainly consisted of alpha helix (69.3-87.4%), beta sheet (27-74.2%), and turns (11-14.7%) (Fig. 3B). Within the

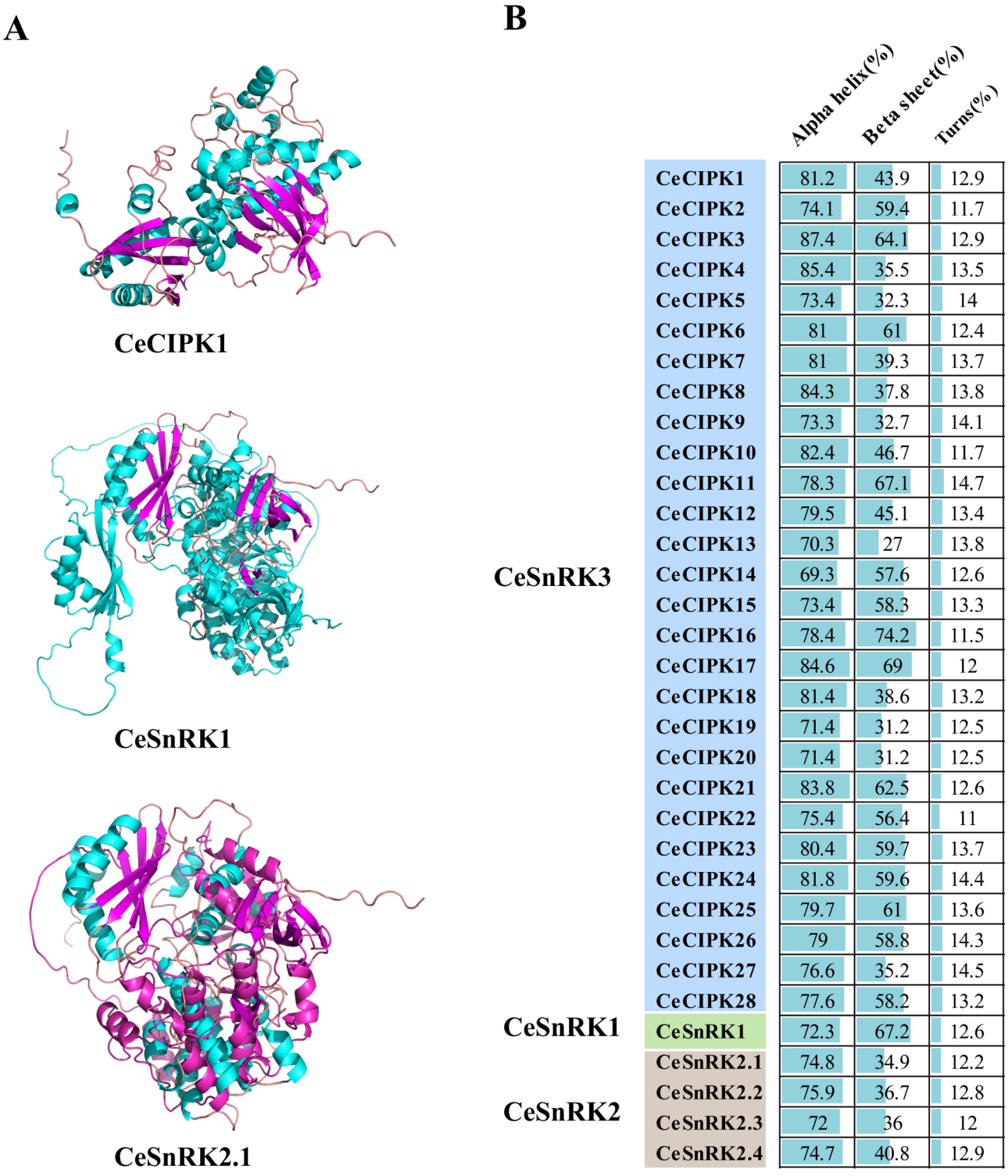

Fig. 3 The prediction protein structures of CeSnRK proteins. **(A)** The protein tertiary structures of representative members from three CeSnRK subfamilys. **(B)** Secondary structure ratio of 33 CeSnRK proteins

secondary structure of CeCIPK3, the proportion of alpha helix was the highest, with CeCIPK16 and CeCIPK11 exhibiting the highest proportions of beta sheet and turns, respectively.

Representative protein sequences from three subfamilies of CeSnRK proteins (CeSnRK1, CeSnRK2.1, CeCIPK1) were selected and submitted to the Alphafold2 software for tertiary structure prediction analysis.

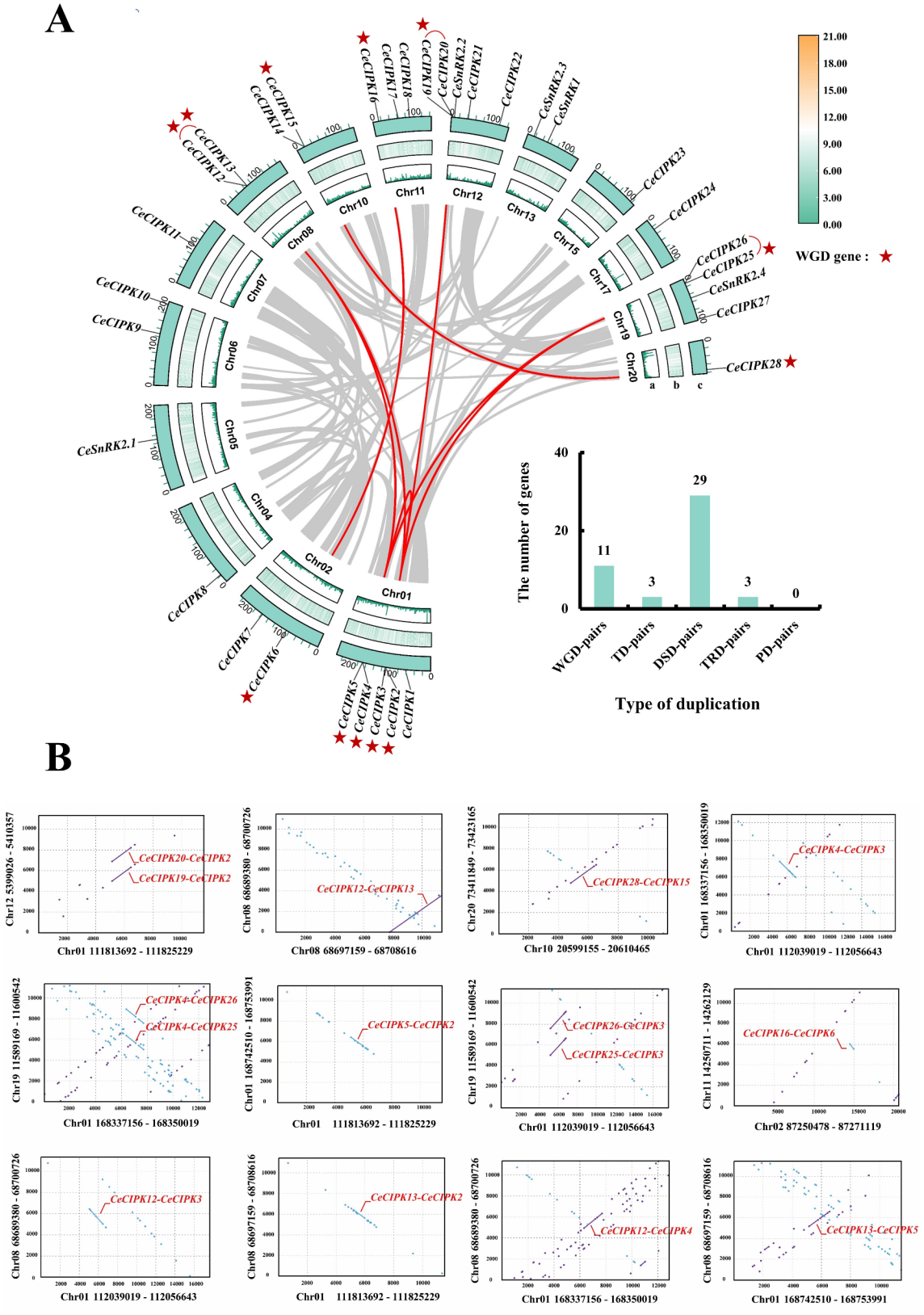

Fig. 4 (See legend on next page.)

(See figure on previous page.)

Fig. 4 Chromosomal locations and synteny of the *CeSnRKs* in the *C.ensifolium* genome. **(A)** The synteny between chromosomes containing *CeSnRK* genes.The red lines inside indicate pairs of *CeSnRKs* involved in duplicated events, while the gray lines indicate duplicated events that occur between chromosomes for other genes.The red lines outside the circular diagram specifically highlight the genes that undergo tandem duplication. The bar chart shows the number of different duplications. WGD-pairs: whole-genome duplication gene pairs, TD-pairs: tandem gene pairs, PD-pairs: proximal gene pairs, TRD-pairs: transposed gene pairs, DSD-pairs: dispersed gene pairs. a: The green line represents gene density. b: The depth of the fragment's color indicates gene density. c: Chr01–Chr20 represents the chromosome representing the presence of *SnRKs* in the *C.ensifolium*. **(B)** The local synteny involving *CeSnRK* genes. Purple and blue represent the positive strand and reverse complement strand, respectively

The results indicated that CeSnRK1, CeSnRK2.1, and CeCIPK1 shared similar proportions of alpha helix and turns, but CeSnRK1 had a higher proportion of beta sheet compared to the other two (Fig. 3A). The tertiary structure of CeSnRK proteins further demonstrated structural differences among members of different subfamilies, highlighting the functional diversity of CeSnRK proteins.

Chromosomal location and synteny analysis of *SnRK*s

To better understand the pattern of gene location, we selected four orchid genomes at the chromosome assembly level to investigate the distribution of *SnRK* genes on chromosomes. Our results showed that *SnRK* genes in each orchid species were unevenly distributed across multiple chromosomes (Supplementary Table S8). The chromosome CM028150.1 of *V. planifolia* had the most *SnRK* genes, with 9, followed by chromosome CM028155.1 with 7. Among the remaining chromosomes of *D. chrysotoxum*, *D. nobile*, and *C. ensifolium*, the maximum number of *SnRK* genes was only 5. The distribution of multiple genes on the same chromosome might be driven by certain duplication events. To explore this further, we conducted an in-depth analysis of the *SnRK* genes in *C. ensifolium*. Chromosome localization results revealed uneven distribution of *CeSnRKs* across *C.ensifolium* chromosomes (Fig. 4). With exceptions on chromosomes 3, 9, 14, 16, and 18, 1 to 5 *CeSnRKs* were dispersed on other chromosomes. Notably, chromosomes 1 and 12 exhibited the highest *CeSnRK* count, each with five members (Fig. 4A). Furthermore, twelve segmental duplication events involving nine genes (*CeCIPK2*, *CeCIPK3*, *CeCIPK4*, *CeCIPK5*, *CeCIPK6*, *CeCIPK12*, *CeCIPK13*, *CeCIPK15*, *CeCIPK16*, *CeCIPK19*, *CeCIPK25*, and *CeCIPK28*) were identified. Annotation data revealed close distances between *CeCIPK12-CeCIPK13*, *CeCIPK19-CeCIPK20*, and *CeCIPK25-CeCIPK26* on chromosomes, might have indicated tandem duplication events (Fig. 4A and B). Additionally, results from DupGen-finder revealed various types of duplication events (Fig. 4A). The most numerous were DSD-pairs, with 29 pairs, while no PD-pairs were identified. Both TRD-pairs and TD-pairs had three pairs each, and WGD-pairs consisted of 11 pairs. The 11 WGD-pairs involved 12 *CeSnRK* genes. Notably, the three gene pairs involved in tandem duplication events all exhibited segmental duplication relationships with *CeSnRK* genes on the Chr01 chromosome. Our results showed that the dispersed duplication was identified as the primary driver for *CeSnRK* expansion.

Cis-acting elements in the promoter region of the *CeSnRK* gene

Analyzing cis-acting regulatory elements within gene promoters provides valuable insights into the tissue-specific or stress-responsive expression patterns of genes. In this study, we meticulously analyzed the 2 kb upstream promoter region of 33 *CeSnRKs* using the PlantPAN online software to uncover their potential regulatory mechanisms (Fig. 5A). A total of 40 transcription factor binding sites were identified, appearing 18,399 times across these promoter regions. The most Ce*SnRK* genes contained elements such as AP2/ERF, AT-hook, TBP, bZip, Homeodomain, GATA, bHLH, Dof, MYB, and NF-Y(A/B/C). These cis-acting elements can divided into three major categories, including temperature-responsive, drought-responsive, and ABA signaling-responsive (Fig. 5B). Notably, we found lots of ABA-responsive elements such as AP2/ERF, AT-Hook, bHLH, bZIP, C2H2, Dehydrin, Dof, Homeodomain, MYB, NAC, and TBP serve as endogenous growth regulators in higher plants. Drought stress-responsive elements included AP2/ERF, bHLH, bZIP, C2H2, Dehydrin, Dof, EIN3; EIL, GATA, HD-ZIP, Homeodomain, HSF, MYB, NAC, NF-YB; NF-YA; NF-YC, SRS, Trihelix, VOZ, WRKY, YABBY, and ZF-HD. Cold and heat stress-responsive elements included AP2/ERF, AT-Hook, bHLH, bZIP, C2H2, Dehydrin, Dof, EIN3; EIL, GATA, Homeodomain, HSF, MYB, SRS, Trihelix, VOZ, and WOX.

CeSnRK2.2 had the highest count of cis-acting elements, totaling 698, followed closely by *CeSnRK2.3* with 679. Conversely, *CeCIPK8* had the fewest cis-acting elements, with only 359. Regarding the types of elements, AP2/ERF and AT-Hook exhibited the highest occurrences, with 2779 and 1846 instances, respectively. In contrast, LFY demonstrated the lowest frequency, with merely 3 occurrences, while GRAS (5) and LOB; LBD (7) also exhibited relatively scarce appearances. Overall, distinct differences were discernible in the distribution of cis-acting elements among members of *CeSnRK* gene family.

The 2000 bp upstream promoter region was divided into distinct segments for clustering analysis (Fig. 5C). The results showed that all *CeSnRK* genes fell into two

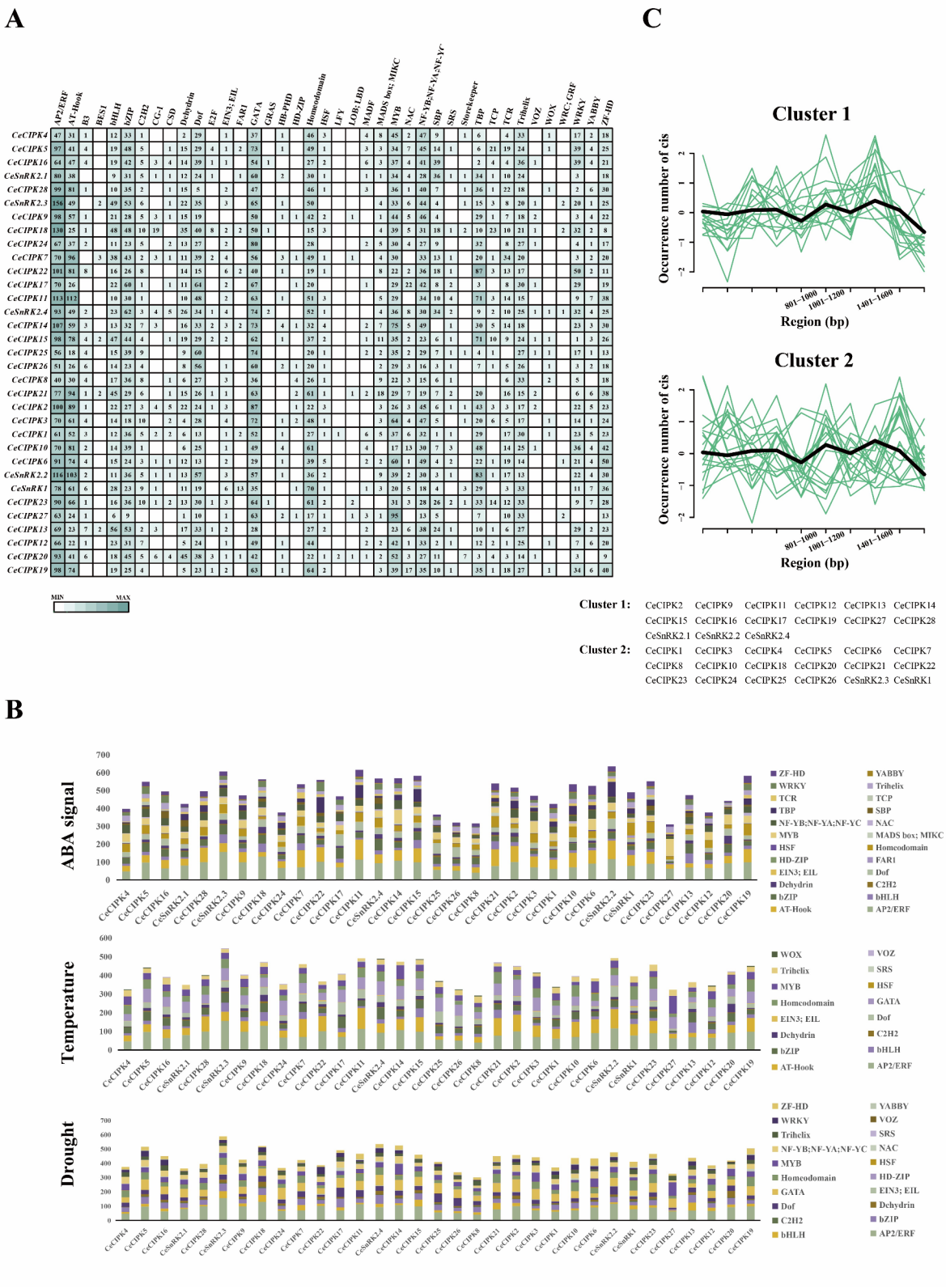

Fig. 5 Analysis of cis-acting elements in *CeSnRK* promoters. **(A)** Heat map illustrating the abundance of cis-acting elements in the *CeSnRK* genes. **(B)** Analysis of cis-acting elements across different response categories (ABA signaling, temperature, drought). **(C)** Clustering analysis of different upstream promoter regions

clusters (Cluster 1 and Cluster 2). The highest clustering was observed in the 1401–1600 bp region for both clusters, while the least clustering occurred in the 1801–2000 bp and 801–1200 bp regions. These clustering results imply that the 1401–1600 bp region may serve as the central area for cis-acting elements.

Expression of *CeSnRKs* in response to ABA

To further elucidate the relationship between *CeSnRKs* and ABA, we examined the expression of 11 highly expressed genes under ABA treatment. The results indicated that all *CeSnRK* genes responded to ABA, with most genes being up-regulated on the third day and down-regulated by the seventh day (Fig. 6). Specifically, *CIPK8*, *CIPK14*, *CIPK15*, *CIPK27*, *SnRK1*, and *SnRK2.1* showed significant expression increases on the third day. Conversely, *CIPK11*, *CIPK24*, *CIPK28*, and *SnRK2.4* displayed initial down-regulation, followed by up-regulation, and then down-regulation again. Additionally, *CIPK20* displayed a notable down-regulation in expression. The active response of *CeSnRKs* to ABA is consistent with the results of cis-element analysis. As core genes in the ABA signaling pathway, the varied expression patterns

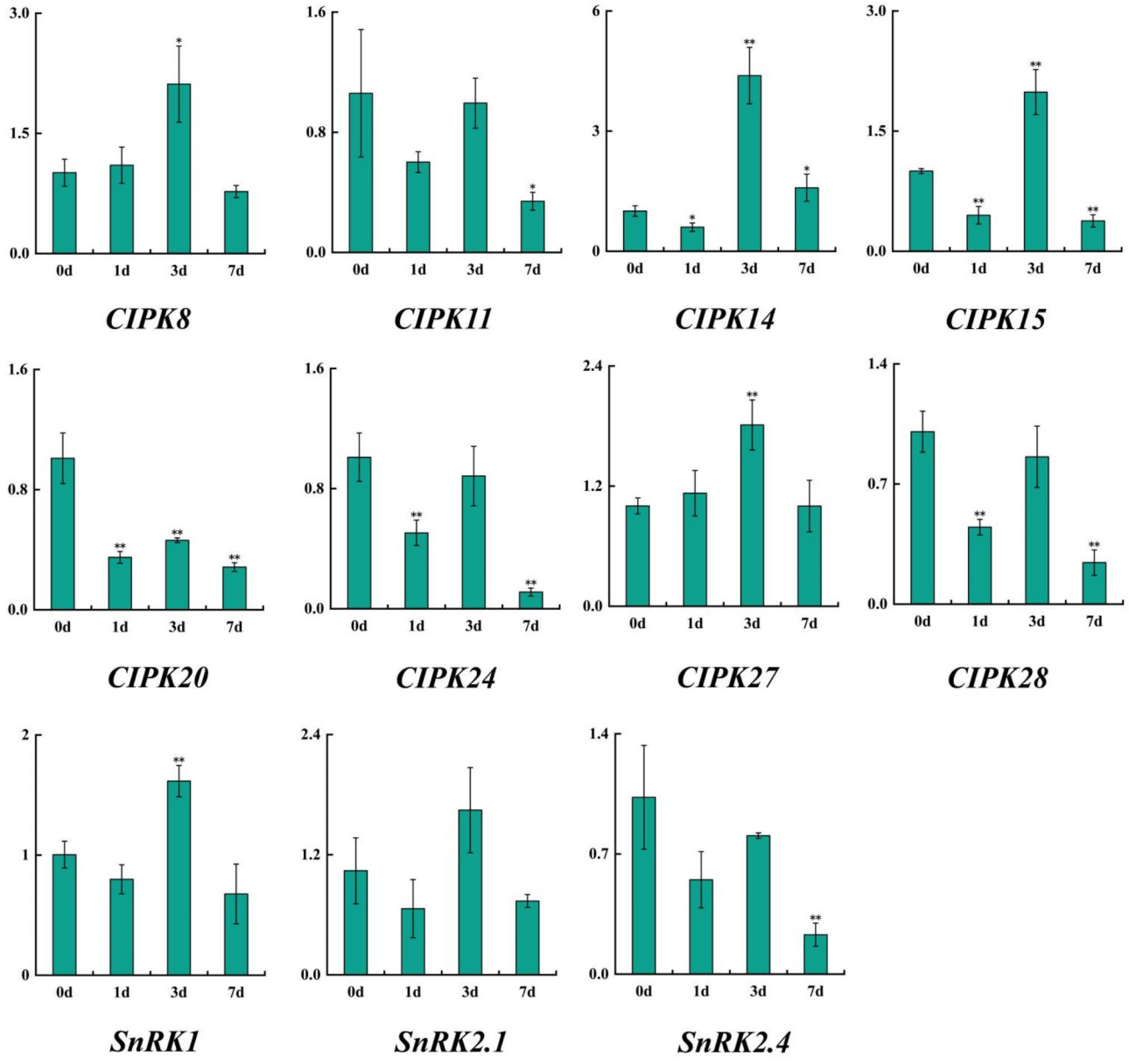

Fig. 6 Expression analysis of the 11 *CeSnRKs* in leaves under ABA treatment. The Y-axis and X-axis represent the relative expression levels and the time courses of stress treatments, respectively. The data represent means ± standard error (SE) of three independent measurements using a t-test, where significance levels were denoted as * for $p < 0.05$ and ** for $p < 0.01$

of different *CeSnRKs* underscore the complexity of *SnRK* gene responses to ABA.

Prediction of MiRNA targets for 33 *CeSnRK* genes

The predicted miRNA binding sites for the 33 members of the *CeSnRK* gene family were detailed in Supplementary Table S3, with representative members from the three subfamilies visually depicted in Fig. 7. The analysis unveiled that all members, except for *CeCIPK18*, harbored two or more miRNA binding sites. Notably, *CeCIPK26* displayed the highest number of miRNA targets, with 17 identified (Fig. 7), closely followed by *CeCIPK5*, which possessed 16 miRNA targets. Conversely, *CeCIPK24* exhibited the fewest miRNA targets, with only two identified. Among all *CeSnRKs*, miR172d-5p and miR414 were the most prevalent, each occurring six times. Following closely was miR838, occurring five times. Several miRNAs associated with abiotic stress were identified in the prediction results. For instance, miR414 was related to growth, development, and water stress, while miR156 was correlated with temperature stress. Additionally, miR165 and miR166 were associated with ABA response, among others. These findings underscored the existence of a complex regulatory network between miRNAs and *CeSnRKs*.

Functions and regulatory networks of CeSnRKs

The three subfamilies of CeSnRK all exhibit conserved domains (Fig. 8), including the serine/ threonine protein kinase active site, ATP binding site, and domain I of CeSnRK2. In addition to the kinase domain, CeSnRK3 also has NAF and PPI domains. These conserved domains provide the basis for CeSnRK to perform various functions. Investigating the regulatory network of gene family was crucial for understanding their biological functions. Therefore, the interaction network of CeSnRK proteins was examined. A total of 40 functional proteins were identified as interactors with CeSnRK proteins (Fig. 8).

Interaction proteins associated with CeSnRKs were categorized into five groups based on their functional roles: ABA signal transduction-related proteins (e.g., ABI1, ABI2, PP2CA, SLAC1, etc.), temperature-related proteins (e.g., CBL1, GORK, CAX1, etc.), salt stress proteins (e.g., CBL3, CBL4, CBL5, CAX1, NHX7, etc.), and drought stress proteins (e.g., AKT1, NPF6.3, PYR1, KAT3, etc.). Additionally, several calcineurin B-like proteins were identified to interact with CeSnRKs, including CBL1, CBL9, CBL2, CBL10, and others. Given the multifunctionality of proteins, some may belong to multiple categories. Notably, 17 proteins were implicated in ABA signal transduction, while only 6 were linked to temperature stress. The Venn diagram results highlighted the involvement of ABI2 in all stress responses. ABI1, ABI2, CBL1, GORK, and PP2CA were implicated in ABA, temperature, and drought stress. The predicted protein-protein interaction (PPI) network elucidated potential CeSnRK interactions in response to abiotic stress.We demonstrated multiple functions of CeSnRK proteins, including phosphorylation, regulation of ABA signaling, and participation in the CBL-CIPK network, among others (Fig. 8). These functions arise from the interaction of specific domains in CeSnRK proteins with related proteins, underscoring the specificity and diversity of CeSnRK protein functions.

Phosphorylation site prediction analysis of the CeSnRK proteins

The NetPhos 3.1 server was utilized to predict phosphorylation sites on CeSnRK proteins, aiming to further elucidate their functions. The results showed a total of 1640 predicted phosphorylation sites across the 33 CeSnRK proteins, comprising 1022 serine, 450 threonine, and 168 tyrosine residues (Fig. 9 and Supplementary Table S4). Among these, CeCIPK5 exhibited the highest number of serine phosphorylation sites, with 57. CeCIPK1 had the highest number of threonine phosphorylation sites, totaling 21, while CeSnRK2.2 had the highest number of tyrosine phosphorylation sites, with 14 (Fig. 9B). Furthermore, the prediction results revealed specific binding sites for 16 protein kinases at phosphorylation sites (Fig. 9A). Among them, PKA, PKC, and CKII kinase binding sites were relatively abundant, with CeCIPK11 and CeCIPK17 each possessing 14 PKC kinase binding sites, the highest among all proteins. CeCIPK5 had the most PKA kinase binding sites, while CeCIPK7 and CeCIPK18 had the most CKII kinase binding sites. The variability in phosphorylation sites further highlights the functional diversity of CeSnRK proteins.

Expression profiles of *CeSnRK* members across different tissues and stages

The expression profiles of the identified 33 *CeSnRK* gene family members in leaf, pseudo-bulb, root and flower were analyzed based on transcriptome data. The results indicated that the majority of *CeSnRK* genes exhibited expression across various tissues and developmental stages of *C. ensifolium*. Notably, *CeSnRK2.1* and *CeCIPK28* exhibited high expression not only in flowers but also in other obtained tissues, notably leaves, pseudo-bulbs, roots, as well as flowers at both initial and decay stages (Fig. 10B and C). In contrast, *CeCIPK22*, *CeCIPK25*, *CeCIPK26*, and *CeCIPK19* exhibited minimal to negligible expression. The majority of genes exhibited specific expression patterns across different developmental stages of the flowers. For instance, *CeCIPK3* displayed maximal expression levels in small buds, with a gradual decline as the buds progressed in growth. In contrast, *CeCIPK8*, *CeCIPK21*, and *CeSnRK1* peaked in expression

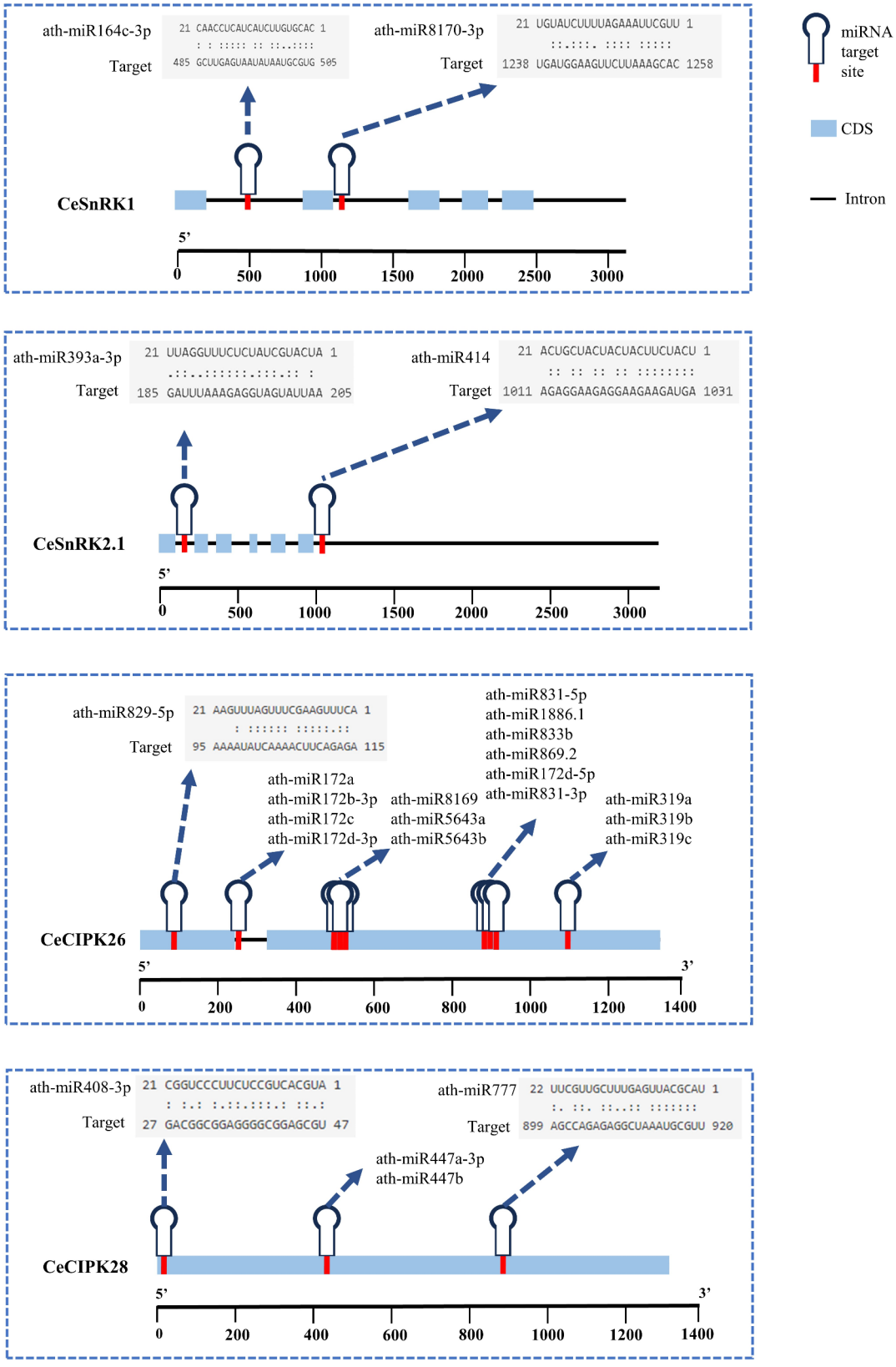

Fig. 7 Prediction of microRNAs target sites for typical *CeSnRK* genes. Each blue dashed box represents a gene fragment, comprising coding sequences (CDS) and introns. Combination of blue rectangular and blue circular elements denote miRNAs, while red rectangles mark the specific binding sites on genes where miRNAs interact, collectively referred to as miRNA binding sites. Blue arrows point to various miRNAs, their sequences, and the sequence of corresponding binding sites on the genes

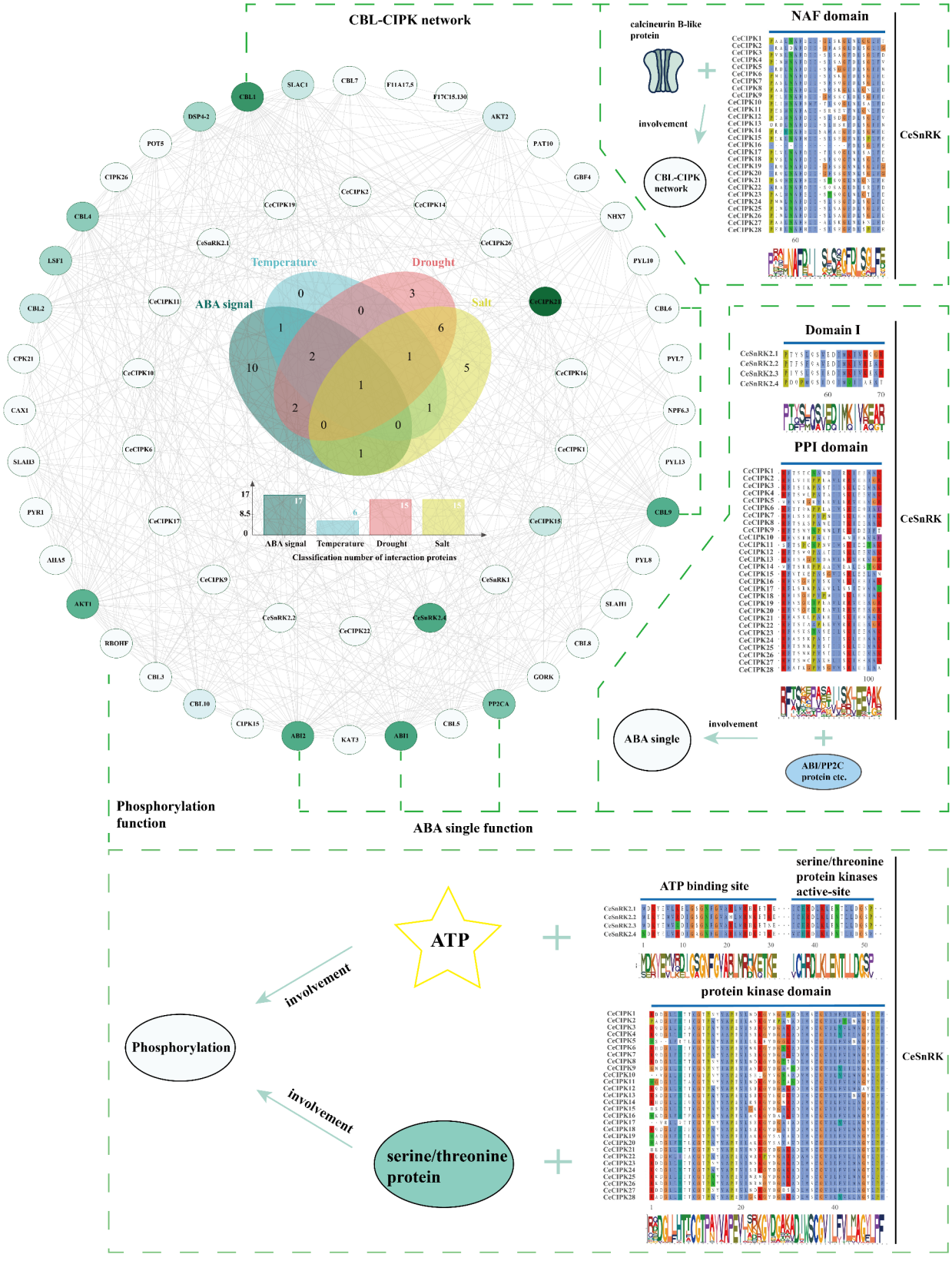

Fig. 8 Predicted protein–protein interaction networks and function description of CeSnRK proteins. The outer circle depicts proteins interacting with CeSnRKs, while the inner circle denotes CeSnRK proteins. The central Venn diagram elucidates the relationships among distinct protein sets, including those related to ABA signaling, temperature response, drought response, and salt response. The bar chart represents the number of four classified proteins. The functional description encompasses the conservative domains, sequence alignments, and associated functions

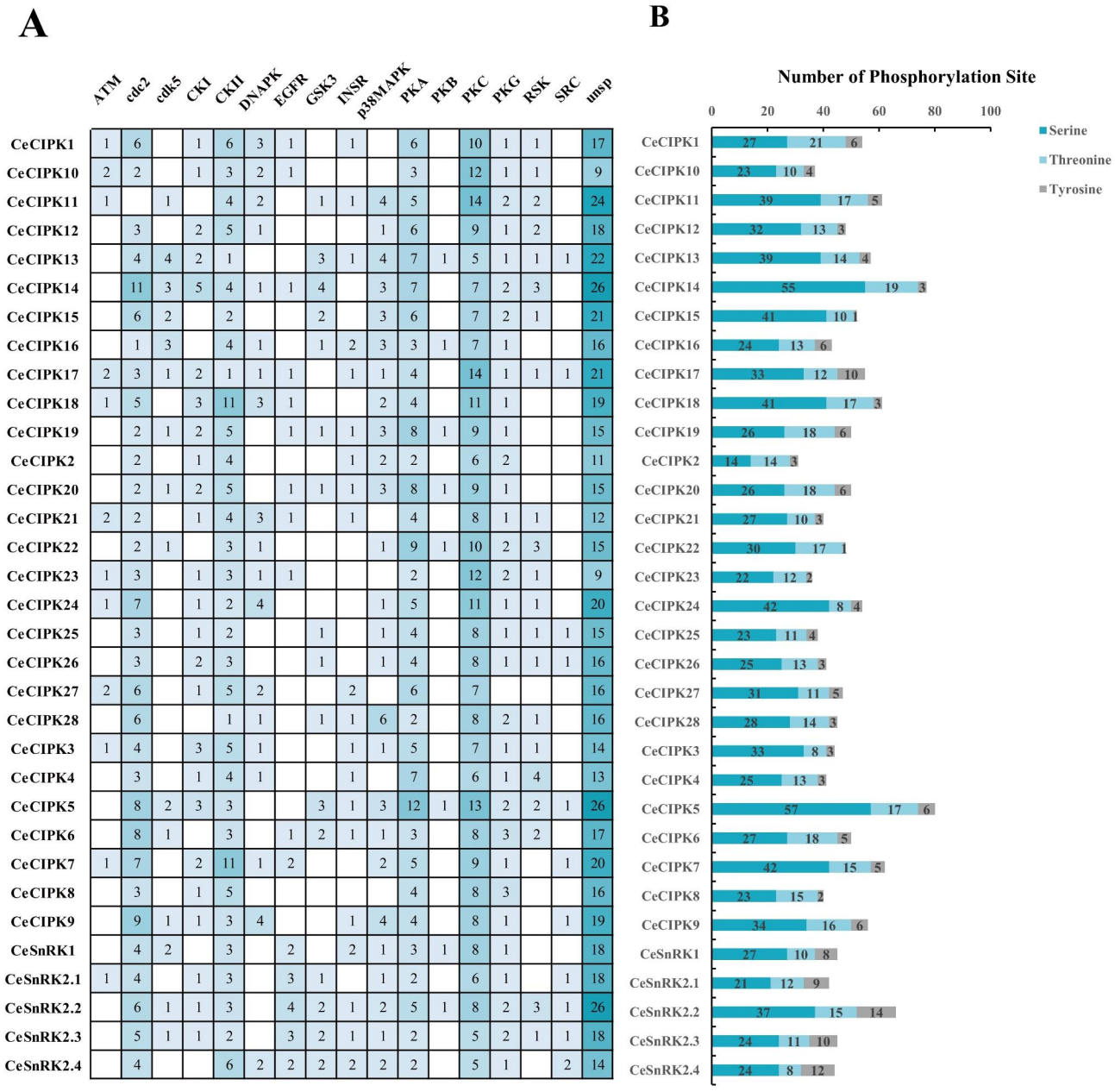

Fig. 9 Phosphorylation Site Prediction Analysis of *C.ensifolium* SnRK Proteins. **(A)** The kinase abundance of 33 CeSnRK protein phosphorylation sites. **(B)** Enumeration of protein phosphorylation sites within CeSnRK proteins

during the initial blooming phase. interestingly, certain genes, such as *CeCIPK28*, *CeCIPK15*, *CeCIPK12*, and *CeCIPK20*, demonstrated heightened expression levels during the senescence stage of the flowers. In roots, pseudo-bulbs, leaves, and floral organs (Fig. 10B and C), *CeCIPK24* and *CeCIPK8* exhibited specific high expression solely in leaves, while *CeCIPK12* showed the most pronounced expression levels in pseudo-bulbs.

To delve deeper into the specificity of gene expression among *CeSnRK* genes, we conducted a gene expression trend analysis (Fig. 10D). Our observations revealed distinct expression patterns: *CeCIPK16*, *CeCIPK11*, and *CeCIPK6* exhibited peak expression levels in leaves, aligning with the expression patterns of *CeCIPK24* and *CeCIPK8* (cluster 5). Cluster 1 and cluster 4 represent tissue-specific expression trends associated with flowers, including *CeSnRK1*, *CeCIPK9*, *CeCIPK23*, etc. Meanwhile, *CeCIPK12* displayed an enhanced expression trend in pseudo-bulbs (cluster 2). Notably, although *CeSnRK2.1* and *CeCIPK28* demonstrated relatively high expression levels across all organs, their most significant expression was noted in roots and pseudo-bulbs (clusters 6 and

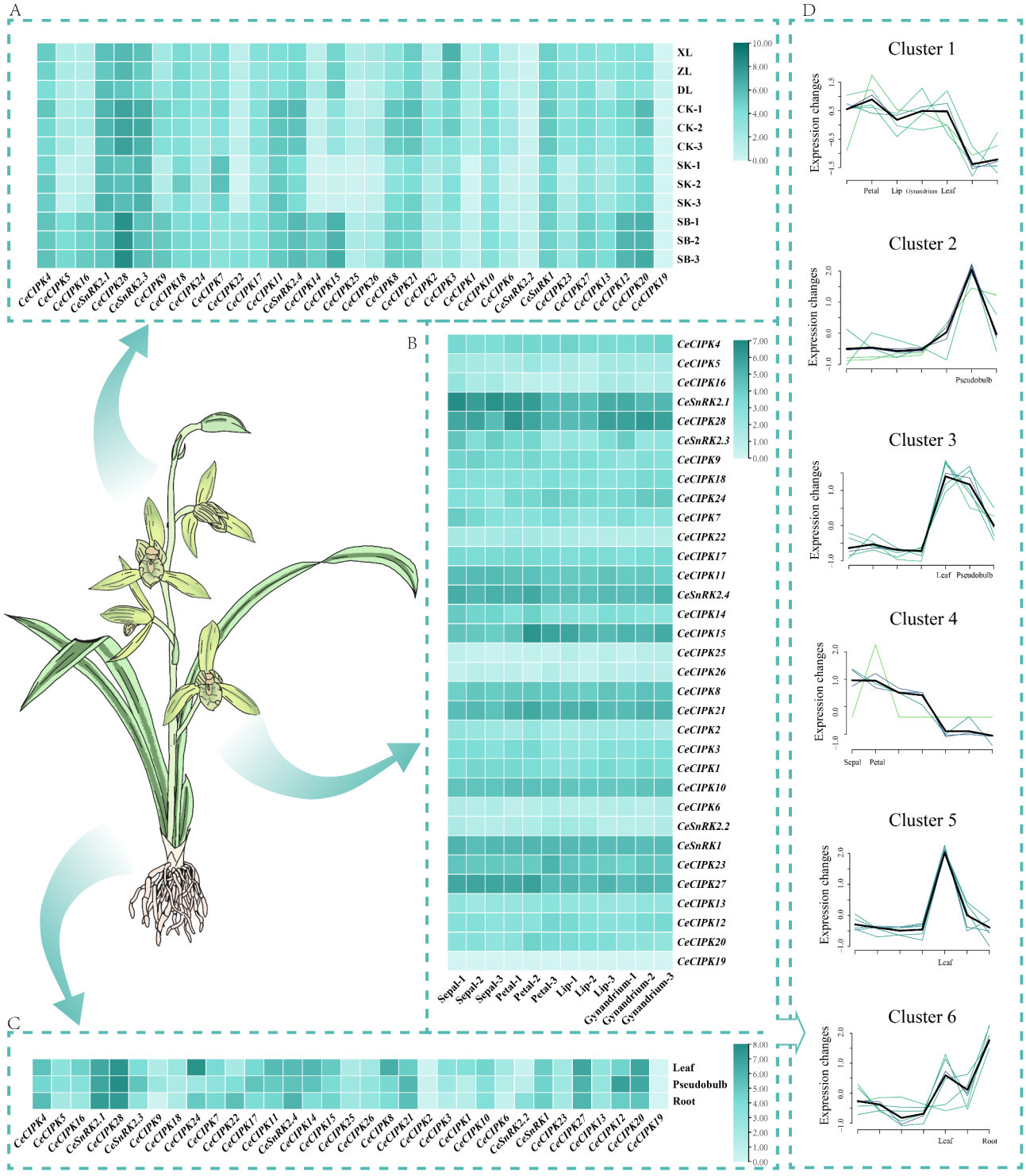

Fig. 10 Heatmap of the expression profiles of the *CeSnRK* gene family. **(A)** Heatmap of the different growth stages of flowers XL: small bud, ZL: middle bud, DL: Mature bud, CK: initially blooming flowers, SK: fully bloomed flowers, SB: decaying flowers. **(B)** Heatmap of different floral organs. **(C)** Heatmap of leaves, pseudobulbs, and roots. **(D)** Gene expression clusteringanalysis of *CeSnRK* genes in indifferent plant tissues. Mfuzz of The OmicStudio tools conducted expression pattern clustering analysis(six clusters)

3, respectively). These trends in gene expression further emphasized the tissue-specific expression patterns of the *CeSnRK* genes.

Expression of *CeSnRKs* in response to drought and low temperatures

Eleven genes, exhibiting relatively higher expression in leaves, pseudo-bulbs, roots, six flower development stages, and floral regions, were identified as target genes. The expression of each gene differed under two treatments (Fig. 11). The majority of genes under PEG 6000 and low-temperature treatment displayed down-regulation. Specifically, some genes treated with PEG6000 showed significant down-regulation (*CIPK11*, *CIPK15*, *CIPK24*, *CIPK28*, and *SnRK2.4*), although *CIPK14* showed an upward trend. In the low-temperature environment, gene expression patterns were similar, with all genes displaying a highly significant down-regulation trend except for *CIPK8*. Notably, *CIPK14* and *CIPK15* were nearly completely suppressed in the cold stress environment. *CIPK14* and *CIPK15* displayed relatively high activity in response to abiotic stresses. Further correlation analysis revealed strong correlations among certain genes, suggesting interconnected expression patterns (*CIPK11*, *CIPK15*, *CIPK27*, *SnRK1*, and *SnRK2.1*). Correlation analysis among the three treatments revealed a positive correlation between ABA treatment and the other two treatments, whereas Cold treatment and drought treatment exhibited a negative correlation. Notably, a strong positive correlation existed between ABA treatment and drought treatment, which was highly significant. This strong positive correlation was consistently observed across multiple genes. For instance, *CIPK14* exhibited up-regulated expression under both ABA and drought treatments, *CIPK27* maintained relatively high expression levels under both conditions, and *SnRK2.4* showed down-regulated expression under both treatments, among others (Figs. 6 and 11).

Materials and methods

Identification and physicochemical properties of *SnRK* genes in orchid genomes

Genome data of *C. ensifolium* [13] were downloaded from the National Genome Data Center (NGDC) (https://ngdc.cncb.ac.cn/, accessed on 10 October 2023). The amino acid sequences of *A. thaliana* and rice SnRK proteins were derived from the databases Tair (https://www.arabidopsis.org/,accessed on 1 March 2024) and Ensymble-plants (https://plants.ensemble.org/,accessed on 1 March 2024). Using the SnRK protein sequences of *A. thaliana* as the query sequence, a BLASTP search was performed on the *C. ensifolium* genome by TBtools-II [54] (Version 2.069, E value $< 1 \times 10^{-5}$, number of hits: 500, number of alignments: 250). The genomic information for the remaining eight orchids (*D. catenatum*, *D. chrysotoxum*, *D. nobile*, *Gastrodia elata*, *Phalaenopsis aphrodite*, *P. equestris*, *Apostasia shenzhenica*, *Vanilla planifolia*) was detailed in Supplementary Table S7. The identification of *SnRK* genes in these species followed the same methodology as described earlier. Domain checking was performed through the sequence alignment function of Phylosuite (version 1.2.3) [55] to remove irrelevant sequences. ProtParam online analytical tools (https://web.expasy.org/protparam/, accessed on 1st March 2024) were employed to predict several protein properties, including the number of amino acids, molecular weight, theoretical pI, instability index, aliphatic index, and grand average of hydropathicity. Broccoli v1.2.1 [56] was used to analyze the orthologous relationships of *SnRK* genes in 9 orchids.

Analysis of phylogenetic relationships, gene structure and conserved domains of *CeSnRKs*

The phylogenetic analysis tree of orchids was derived from previous research [57]. Neighbor-joining (NJ) phylogenetic trees of *A. thaliana*, rice and *C. ensifolium* were constructed using PhyloSuite (Version 1.2.3) with 1000 bootstrap replicates and visualized on the iTOL website (https://itol.embl.de/, accessed on 2nd March 2024). MEME (https://memesuite.org/meme/doc/, accessed on 2nd March 2024) was used to analyze conserved motifs, and multiple sequence alignments were visualized with OmicsSuite (Version 1.4.0) [58].

Prediction of secondary and tertiary structures of the CeSnRKs

The CFSSP database (https://www.biogem.org/tool/chou-fasman/, accessed on 3 March 2024) was used to analyze secondary structure, while Alphafold2 (https://colab.research.google.com/github/sokrypton/ColabFold/blob/main/AlphaFold2.ipynb, accessed on 3 March 2024) was used to predict the tertiary structure of 33 CeSnRK proteins. The tertiary structure of the protein was visualized using PyMOL (Version 2.5.7).

Chromosomal localization and gene duplication

According to the genome annotation, all *CeSnRK* genes were mapped to their respective chromosomes. Their duplication events were analyzed using MCScanX [59] and Dupgen-finder [60], with default parameters. Identification of Tandem duplication and Segmental duplication followed previous research [61–63].The Advanced Circos and Dual Synteny Plot of TBtools-II (Version 2.069) were employed for visualization. Genome fragments were extracted using TBtools-II (Version 2.069) and local synteny analysis was performed using MUMmer (Version 4) [64]. Visualization was accomplished using mummerplot.

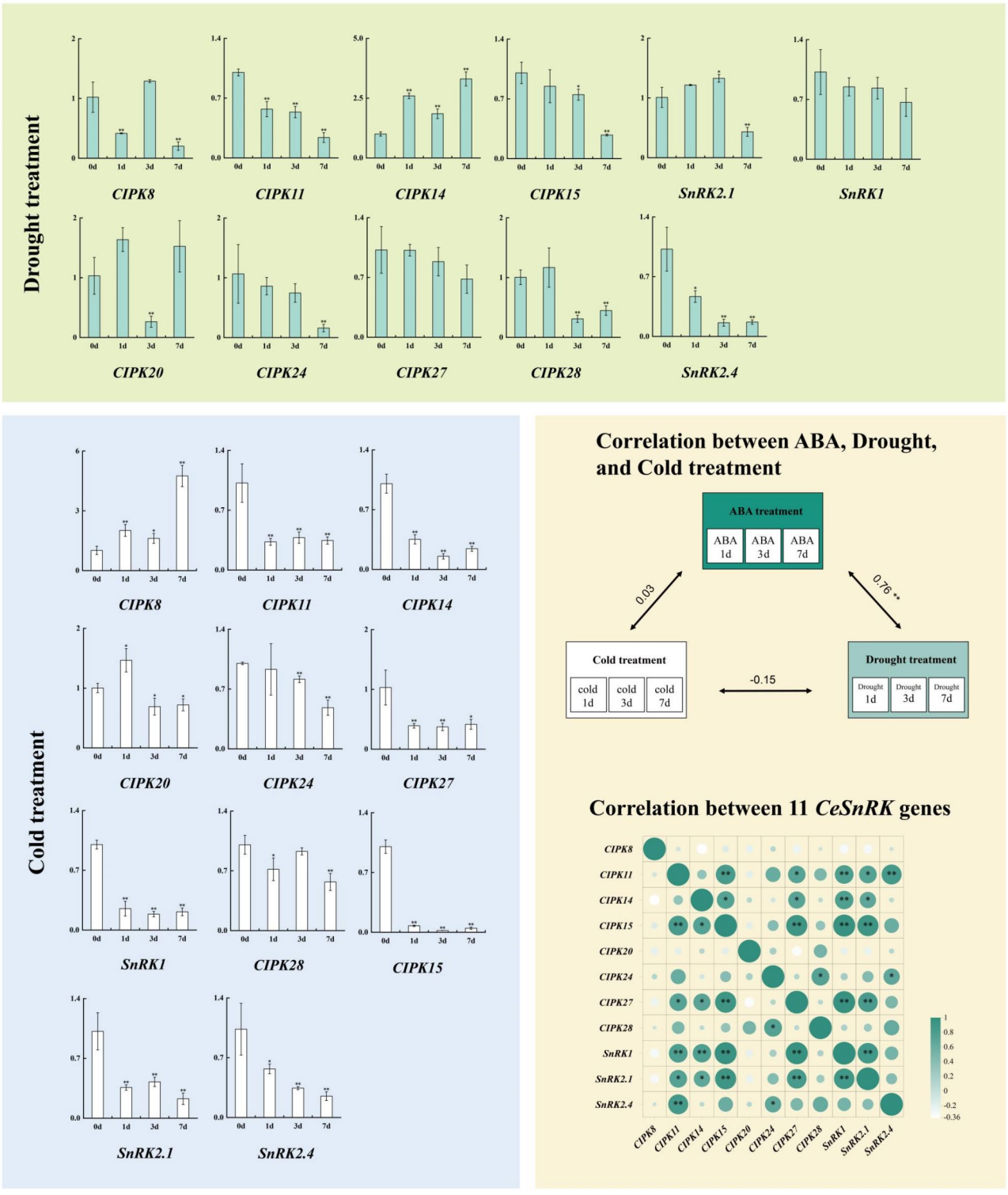

Fig. 11 Expression analysis of the 11 *CeSnRKs* in leaves under various abiotic stresses (drought and low-temperature treatments). The Y-axis and X-axis represent the relative expression levels and the time courses of stress treatments, respectively. A heatmap illustrated the correlation of gene expressions between the three treatments. A correlation diagram base on gene expressions illustrating the correlation among three different treatments. The data represent means ± standard error (SE) of three independent measurements using a t-test, where significance levels were denoted as * for $p < 0.05$ and ** for $p < 0.01$

Prediction of cis-acting elements and miRNAs binding sites in *CeSnRKs*

The sequences of the upstream 2,000 bp region of the *C. ensifolium SnRK* gene were retrieved from the start codon using TBtools-II (Version 2.069) software. The cis-acting elements within the *SnRK* promoter region were investigated using PlantPAN4.0 (http://plantpan.itps.ncku.edu.tw/plantpan4, accessed on 5th March 2024). Mfuzz analysis was conducted using OmicStudio tools (https://www.omicstudio.cn/tool, accessed on 5th March 2024). The psRNATarget database was utilized to predict miRNA binding sites within the 33 *CeSnRK* genes [65]. Data analysis and visualization were conducted using Excel 2021 and PowerPoint 2021.

The prediction of protein-protein interaction network and phosphorylation site in CeSnRKs

We used to the STRING database (https://cn.string-db.org/, accessed on 5th March 2024) to predict protein interaction networks. This network comprised 33 CeSnRK protein sequences, with reference to *A. thaliana*, and considered up to of 20 interactors spanning the 1st and 2nd shells. Subsequently, the protein interaction network of CeSnRKs was visualized using Cytoscape (version 3.9.1) [66]. Node colors were assigned based on their respective degrees and betweenness using continuous mapping. Nodes with higher degrees were depicted in darker colors. The phosphorylation sites of CeSnRK proteins were predicted through the NetPhos-3.1 database (https://services.healthtech.dtu.dk/services/NetPhos-3.1/, accessed on 3th March 2024) and visualized with EXCEL2021.

The assay of RT-qPCR and gene expression patterns analysis

To explore the potential involvement of *SnRK* genes in various tissues of *C. ensifolium*, we obtained the RNA-seq data of *C. ensifolium* from the National Genomics Data Center. Genome Sequence Archive (GSA) RUN accession numbers were presented in Supplementary Table S5. The calculation method for TPM (Transcripts Per Million) values of *C. ensifolium SnRK* genes referenced previous articles [49]. The data were visualized using TBtools-II (version 2.069). Mfuzz analysis was conducted using OmicStudio tools (https://www.omicstudio.cn/tool, accessed on 5 March 2024). Experimental materials were sourced from the germplasm nursery of Fujian Agriculture and Forestry University, where the *C. ensifolium* variety 'Xiao Tao Hong' was cultivated. Each treatment included three biological replicates, with untreated plants exhibiting similar growth conditions serving as the control group. Polyethylene glycol (PEG) 6000 is a good reagent to simulate drought for plant and has been widely used in many studies [67]. Plants underwent treatments with 20% PEG 6000 for drought [68–71], 100μM abscisic acid (ABA), and 4°C for low-temperature treatments [72]. Following 1, 3, and 7 days of these treatments, individual leaves of 'Xiao Tao Hong' were sampled. Samples were collected in 1.5 mL sterile non-enzymatic cryopreservation tubes and stored in a -80 °C refrigerator. Experimental procedures for total RNA extraction, reverse transcription, and RT-qPCR were consistent with previous references [49, 73]. The *CeTUB* gene served as the internal reference. The sequences of the 11 genes and internal reference primers used in the reaction were provided in Supplementary Table S6. Gene expression levels were analyzed using the $2^{-\Delta\Delta Ct}$ method, with data processed using one-way analysis of variance (ANOVA) [74]. Statistical differences and visual analyses were conducted using Origin and Chiplot (https://www.chiplot.online/, accessed on 3th April 2024). Correlations among the three distinct treatments were computed and visualized using R version 4.3.3 and RStudio version 2023.12.1.

Discussion

Variations in *SnRK* genes among different species of Orchidaceae

The *SnRK* gene family is a pivotal group of protein kinases in plants, playing significant roles in plant growth under stress conditions, and in the response of plants to abiotic stress and ABA signaling [75, 76]. Consequently, researchers have extensively investigated the *SnRK* gene family. Previous reports identified varying numbers of *SnRK* genes in different plant species, such as 34, 48, 44, and 60 in *Eucalyptus grandis* [77], rice [78], *Brachypodium distachyon* [19], and *Hedychium coronarium* [79], respectively. However, there were relatively few investigations have been conducted on *SnRK* genes in orchids. This study systematically identified *SnRK* genes from nine orchids and conducted a comprehensive exploration of the *SnRK* genes in *C. ensifolium*. The number of *SnRK* genes in these nine species of Orchidaceae ranged from 30 to 64, with most orchids possessing between 30 and 41 members, underscoring the conservation of *SnRK* genes in orchids. Notably, *P. equestris* (64) and *D. catenatum* (51) exhibited the highest numbers of *SnRK* genes, which could be linked to whole-genome duplication events in monocotyledonous plants and orchids [13, 80]. Furthermore, all nine orchids harbored *SnRK* genes classified into three subfamilies, with most species having a single member in the SnRK1 subfamily, consistent with prior findings [31]. Leveraging the genomic data of *C. ensifolium*, we identified 33 *CeSnRK* genes, which were classified into three subfamilies through phylogenetic analysis (Fig. 1B). There were 1, 4, and 28 *CeSnRK* genes in the CeSnRK1, CeSnRK2, and CeSnRK3 subfamilies, respectively. Similar to the other eight orchids, the CeSnRK3 subfamily exhibited the highest number

of members. While CeSnRK3 subfamily displayed considerable sequence conservation (Fig. 8), some family members showed expansion, likely associated with WGD events (Figs. 1B and 4). Although there was a degree of conservation in *SnRK* genes across different habitats of orchids, variations in the number of *SnRK* family members between different species may be attributed not only to WGD events but also to retained differences in the evolutionary process to adapt to diverse environments.

As revealed by sequence analysis (Fig. 8), distinct conserved domains are evident in different *SnRK* gene subfamilies, yet the N-terminal protein kinase domain remains conserved across the entire family. Notably, an NAF domain was identified in the C-terminus of the CeSnRK3 subfamily. Previous studies have demonstrated that the NAF domain interacts with calcineurin B-like proteins, suggesting potential interactions between genes in the CeSnRK3 subfamily and *CBLs* to respond to stress [26, 81]. To delve deeper into the structure of *CeSnRKs*, an analysis of conserved motifs and gene structures was conducted across 33 *CeSnRK* genes. Introns, known to play crucial roles and potentially possess functions independent of their coding genes [82]. The number and distribution of exons/introns in *CeSnRK* genes varied, genes within the same subfamily typically shared similar gene structures. Furthermore, *CeSnRKs* could be categorized into two groups based on intron abundance: intron-rich and intron-poor (Fig. 2B). This differentiation, particularly prominent in the CeSnRK3 subfamily, mirrors observations in the HcSnRK3 subfamily genes [79]. During evolution, populations tend to lose introns, resulting in intron-poor genes from intron-rich ancestors [83]. Intriguingly, a majority (21 out of 28) of CeSnRK3 subfamily genes lacked introns, suggesting a tendency for intron loss within this subfamily. Additionally, motif analysis results (Fig. 2A and C) revealed that all CeSnRK members shared common motifs such as motifs 4, 3, 2, 7, and 1. Moreover, members within the same subfamily exhibited consistent conserved motifs, such as the unique motif 15 in the CeSnRK2 subfamily. These conserved motifs likely play pivotal roles in CeSnRK function. The observed differences in exon/intron structures and motif distribution among various subfamilies underscore the functional diversity of *CeSnRK* genes.

Regulations before and after transcription process led to multiple biological responses

When plants respond to abiotic stress, cis-acting elements activate stress resistance genes by binding to transcription factors [84, 85]. For instance, *GmSnRK2.16* and *GmSnRK2.18* in soybean respond to salt stress [86]. This study analyzed the 2.0 kb upstream promoter region of 33 *CeSnRK* genes, identifying 40 transcription factor binding sites (Fig. 5). The most prevalent transcription factor, AP2/ERF, was associated with ABA signaling, drought stress, and temperature stress [87, 88]. These cis-acting elements were categorized into three groups: ABA signaling, drought, and temperature-related, comprising 24, 20, and 16 transcription factors, respectively. ABA signaling elements predominated, suggesting widespread involvement of *CeSnRK* genes in ABA response. Cluster analysis identified the 1401–1600 bp region as the core area for cis-acting elements (Fig. 5). Within this core region, AP2/ERF elements were the most abundant, followed by AT-hook elements known to respond to cold stress in *Poncirus trifoliata* (L.) Raf [89]. These findings highlighted the significant role of *CeSnRK* genes in responding to various abiotic stresses, including cold stress, in *C. ensifolium*. The presence of cis-acting elements for various stresses in *C. ensifolium SnRK* genes implied their participation in diverse stress responses. Besides cis-acting elements, miRNA was also involved in plant stress response [90, 91]. Our analysis predicted 133 miRNA binding sites (Supplementary Table S3), including miR165 and miR166 associated with ABA response [92], and miRNA156 related to drought, temperature, and salt stress [93]. MiRNA408 plays a role in plant development and responses to diverse abiotic stresses such as cold, oxidative stress, and drought [94, 95]. It was also predicted to target *CeCIPK28* in this study (Fig. 7). This suggested potential binding of *CeSnRKs* to miRNA for regulating plant stress responses.

Plant growth and stress responses typically rely on complex regulatory networks, including protein interaction networks. Previous studies have demonstrated that plants regulated various physiological activities through protein interactions. For example, interaction between MdBT2 and MdRGL3a regulated salt-mediated plant growth, and TaHSP17.4 interacted with TaHOP to enhance plant stress resistance [96, 97]. Analysis of protein interaction networks revealed interactions between 40 proteins and CeSnRKs, categorized into ABA signaling, temperature, drought, and salt-related proteins (Fig. 8). The prominence of ABA signaling-related proteins further underscored the potential involvement of CeSnRK in ABA response. Interactions with other protein types suggested *C. ensifolium* SnRK proteins' participation in diverse stress responses. The CBL-CIPK network was crucial for plant growth and stress adaptation [98]. Multiple CBL proteins, including CBL1, CBL4, CBL9, interacted with CeSnRK, indicating the potential participation of CeSnRK in the CBL-CIPK network, affecting plant growth and stress adaptation. Previous research indicated that SnRK proteins engaged in various regulatory networks via specific structural domains. The NAF domain of SnRK proteins interacted with calcineurin B-like proteins, participating in the CBL-CIPK network [26, 39]. The PPI domain and Domain I of

SnRK proteins associated with ABI and PP2C proteins in response to ABA signaling [25, 99]. Moreover, SnRK proteins possessed phosphorylation capabilities [18]. Our protein interaction prediction results highlighted strong interactions with CBL proteins, ABI, and PP2C proteins. This suggested that CeSnRK proteins in *C. ensifolium* might have participated in multiple regulatory networks. Post-translational, additional modifications such as phosphorylation were necessary for proper protein function [100]. Protein phosphorylation played a vital role in plant development and environmental response. For instance, SlBBX17 phosphorylation positively regulated tomato cold tolerance [101]. Our results revealed abundant phosphorylation sites in CeSnRK proteins, with multiple kinase binding sites, including CKII and MAPK, predicted (Fig. 9). These kinases improved plant target genes' functionality post-modification. For example, CKII-modified AtYY1 regulated *A. thaliana* ABA response [102], and Populus MKK2a participated in MAPK signaling cascades, affecting plant salt tolerance [103]. The numerous phosphorylation sites emphasized the critical role of *CeSnRK* in responding to abiotic stresses like ABA and salt stress.

The analysis of gene expression patterns revealed varying degrees of expression across different developmental stages and tissues of *C. ensifolium*. Previous studies have highlighted the essential roles of *SnRK* genes in promoting meristematic tissue development and overall plant growth [104, 105]. Genes such as *CeCIPK28*, *CeCIPK15*, *CeCIPK12*, and *CeCIPK20* exhibited high expression levels during flower development. *CeSnRK2.3* showed elevated expression from the initial flower opening stage, gradually decreasing thereafter (Fig. 10A). These results showed that potential involvement in flower development processes. Notably, Tissue-specific expression of *CeSnRKs* was observed in different tissues (Fig. 10B and C), with *CeSnRK2.1* specifically expressed in roots and *CeCIPK28* in pseudobulbs. Tissue-specific expression was also observed in leaves, petals, and other tissues, suggesting the diverse functions of *CeSnRK* genes across various organs. To explore gene expression responses to different stresses, 33 *CeSnRK* genes were subjected to drought, abscisic acid, and temperature treatments (Figs. 6 and 11). The activation of *SnRK* genes, transitioning from an inactive dephosphorylated state to an active state, was crucial in plant responses to ABA and environmental stresses [106]. Multiple genes showed upregulation under ABA treatment, including *SnRK1*, *SnRK2.1*, and *CIPK14*, particularly on the third day of treatment, consistent with previous findings [107]. The upregulation of *CeSnRK* genes under ABA treatment underscores their crucial role in the ABA response in *C. ensifolium*. Predictions of cis-acting elements and protein interaction networks also reinforce the involvement of *CeSnRK* genes in ABA response. Our results illustrated that *SnRK* genes were involved in the ABA signaling response of *C. ensifolium*. Besides responding to ABA signals, *SnRK* genes also reacted to various abiotic stresses. Prior research has indicated that the RAF-SnRK2 kinase cascade governed signal transduction in plants under osmotic stress, and SnRK2 genes facilitate ABF2 phosphorylation to respond drought stress [108, 109]. Our results revealed that *SnRK2.1* upregulation occurred during the initial 0–3 days of drought treatment. Additionally, genes such as *SnRK1* and *CIPK27* exhibited elevated expression levels. These findings implied that *CeSnRK* genes might share similar signaling and regulatory mechanisms to assist *C. ensifolium* in drought adaptation. Conversely, *CIPK11* and *SnRK2.4* showed downregulation under drought conditions. The significance of this downregulation in drought response warranted further investigation. Consistent with previous research, *SnRK* genes showed differential expression under drought and cold stress [110, 111]. Under cold treatment, *CIPK28* was upregulated, while *SnRK1* and *SnRK2.4* were downregulated. The differential expression patterns of *CeSnRK* genes in response to cold stress indicated their potential role in *C. ensifolium*'s adaptation to cold environments. Many stress responses mediated by *SnRK* are associated with ABA signaling [106]. Thus, we examined the correlation between various stress treatments (Fig. 11). The findings reveal a significant positive correlation between ABA and drought treatments, suggesting that *CeSnRK* genes in *C. ensifolium* might react to stress conditions via ABA signaling. Overall, these findings indicate the complex regulatory roles of *CeSnRK* genes under diverse stress conditions.

Conclusions

SnRK genes play a crucial role in ABA signaling pathways, particularly in response to abiotic stresses. In this study, we identified 362 *SnRK* genes across nine species of Orchids, including 33 in *C. ensifolium*, categorizing them into three main subfamilies with distinct gene structures and motif compositions. Dispersed duplication was identified as the primary driver for *CeSnRK* expansion. Our analysis of cis-acting elements, miRNA binding sites, and protein interaction networks reveals *CeSnRKs* were associated with various stress responses by involvement in the ABA signaling pathway. Besides, member expansion led to tissue-independent expression and function differentiation. The differential expression of *CeSnRK* genes under cold and drought stress indicated a positive response to abiotic stress. These findings significantly deepened our understanding of the role of *SnRK* genes in abiotic stress responses in orchids, particularly the response mechanisms of *SnRK* genes to different stresses. It also provided valuable insights into

the function of *SnRK* genes in plants and supported the future breeding of *C. ensifolium*.

Supplementary Information

The online version contains supplementary material available at https://doi.org/10.1186/s12870-025-06280-9.

Supplementary Material 1: File S1. The CDS sequences of ***CeSnRK*** genes.

Supplementary Material 2: Table S1. 1A Orthologous pairs of ***SnRK*** genes among different orchids; 1B Orthologous groups of ***SnRK*** genes among different orchids.

Supplementary Material 3: Table S2. Protein information of ***SnRK*** gene family in ***Cymbidium ensifolium***. Including gene id, gene name, genomics position and protein aphysicochemical properties.

Supplementary Material 4: Table S3. Results of predicting miRNA targets that regulated genes in different ***CeSnRKs.***

Supplementary Material 5: Table S4. The raw data for the phosphorylation prediction of 33 CeSnRK proteins.

Supplementary Material 6: Table S5. The TPM values of ***SnRK*** genes in ***C. ensifolium.***

Supplementary Material 7: Table S6. RT-qPCR primers used in ***C. ensifolium*** 'Xiao Tao Hong' experiments.

Supplementary Material 8: Table S7. Accession numbers of genome data from different species of Orchidaceae.

Supplementary Material 9: Table S8. Chromosome distribution of ***SnRK*** genes in four orchids.

Author contributions

Y. Z.: Writing – review & editing, Writing – original draft, Supervision, Funding acquisition, Data curation, Conceptualization. D. P.: Writing – review & editing, Supervision, Conceptualization. K. Z.: Writing – review & editing, Writing – original draft, Supervision, Conceptualization. Z.-J. L.: Writing – review & editing, Resources. R. Z.: Writing – original draft, Visualization, Data curation. J. C.: Writing – original draft, Data curation. X. Z.: Writing – original draft, Visualization. Y. P.: Writing – original draft, Data curation. M. S.: Writing – original draft, Data curation. All authors have read and agreed to the published version of the manuscript.

Funding

The Project of National Key R & D Program (2023YFD1600504), Fujian Provincial Natural Science Foundation of China (2023J01283, 2022J01639), the National Natural Science Foundation of China (No. 32101583, 31901353), the Innovation and Application Engineering Technology Research Center of Ornamental Plant Germplasm Resources in Fujian Province (No. 115-PTJH16005), the key research and development program of the Ningxia Hui Autonomous Region in China (2022BBF02041).

Data availability

The raw genome data and assembled C. ensifolium genome was submitted to National Genomics Data Center (NGDC) database with the accession number PRJCA005355/CRA004327 and GWHBCII00000000. The raw transcriptome sequences have been deposited in BioProject of GSA under the accession codes PRJCA009885/CRA007101 and PRJCA005426/CRA004351, respectively. All data generated or analyzed during this study are included in this published article (Supplementary Files) and also available from the corresponding author on reasonable request.

Declarations

Ethics approval and consent to participate

All the plants used in this study were collected and bred in the key laboratory of national forestry and grassland administration for orchid conservation and utilization, Fujian Agriculture and Forestry University, Fuzhou, China. The sample collection and processing methods were permitted by the laboratory and carried out according to the requirements of the local government and international guidelines.

Institutional review board

Not applicable.

Informed consent

Not applicable.

Competing interests

The authors declare no competing interests.

Received: 25 June 2024 / Accepted: 19 February 2025
Published online: 03 March 2025

References

1. Kopecká R, Kameniarová M, Černý M, Brzobohatý B, Novák J. Abiotic stress in crop production. Int J Mol Sci. 2023;24(7).
2. Naing AH, Kim CK. Abiotic stress-induced anthocyanins in plants: their role in tolerance to abiotic stresses. Physiol Plant. 2021;172(3):1711–23.
3. Gong Z, Xiong L, Shi H, Yang S, Herrera-Estrella LR, Xu G, Chao D-Y, Li J, Wang P-Y, Qin F, et al. Plant abiotic stress response and nutrient use efficiency. Sci China Life Sci. 2020;63(5):635–74.
4. Markham KK, Greenham K. Abiotic stress through time. New Phytol. 2021;231(1):40–6.
5. Wang S, Zhou H, Hua G, Wu Q. What is the relationship among environmental pollution, environmental behavior, and public health in China? A study based on CGSS. Environ Sci Pollut Res Int. 2021;28(16):20299–312.
6. Sun S, Sang W, Axmacher JC. China's National nature reserve network shows great imbalances in conserving the country's mega-diverse vegetation. Sci Total Environ. 2020;717:137159.
7. Yang Y, Zhao N, Wang Y, Chen M. Variations in summertime compound heat extremes and their connections to urbanization in China during 1980–2020. Environ Res Lett. 2022;17(6):064024.
8. Wang Z, Li Z, Zhan H, Yang S. Effect of long-term saline mulched drip irrigation on soil-groundwater environment in arid Northwest China. Sci Total Environ. 2022;820:153222.
9. Zhang Q, Shi R, Singh VP, Xu C-Y, Yu H, Fan K, Wu Z. Droughts across China: drought factors, prediction and impacts. Sci Total Environ. 2022;803:150018.
10. Li W, Sun J, Zhang X, Ahmad N, Hou L, Zhao C, Pan J, Tian R, Wang X, Zhao S. The mechanisms underlying salt resistance mediated by exogenous application of 24-Epibrassinolide in peanut. Int J Mol Sci. 2022;23(12).
11. Zhao H, Mallano AI, Li F, Li P, Wu Q, Wang Y, Li Y, Ahmad N, Tong W, Li Y, et al. Characterization of CsWRKY29 and CsWRKY37 transcription factors and their functional roles in cold tolerance of tea plant. Beverage Plant Res. 2022;2(1):1–13.
12. Wang M-J, Ou Y, Li Z, Zheng Q-D, Ke Y-J, Lai H-P, Lan S-R, Peng D-H, Liu Z-J, Ai Y. Genome-Wide identification and analysis of bHLH transcription factors related to anthocyanin biosynthesis in Cymbidium ensifolium. Int J Mol Sci. 2023;24(4).
13. Ai Y, Li Z, Sun W-H, Chen J, Zhang D, Ma L, Zhang Q-H, Chen M-K, Zheng Q-D, Liu J-F, et al. The Cymbidium genome reveals the evolution of unique morphological traits. Hortic Res. 2021;8(1):255.
14. Wang H-Z, Lu J-J, Hu X, Liu J-J. Genetic variation and cultivar identification in Cymbidium ensifolium. Plant Syst Evol. 2011;293(1):101–10.
15. Zhang D, Zhao X-W, Li Y-Y, Ke S-J, Yin W-L, Lan S, Liu Z-J. Advances and prospects of Orchid research and industrialization. Hortic Res. 2022;9:uhac220.
16. Bohnert HJ, Gong Q, Li P, Ma S. Unraveling abiotic stress tolerance mechanisms–getting genomics going. Curr Opin Plant Biol. 2006;9(2):180–8.
17. Hunter T. Protein kinases and phosphatases: the Yin and Yang of protein phosphorylation and signaling. Cell. 1995;80(2):225–36.
18. Son S, Park SR. The rice SnRK family: biological roles and cell signaling modules. Front Plant Sci. 2023;14:1285485.
19. Wang L, Hu W, Sun J, Liang X, Yang X, Wei S, Wang X, Zhou Y, Xiao Q, Yang G, et al. Genome-wide analysis of SnRK gene family in Brachypodium distachyon and functional characterization of BdSnRK2.9. Plant Sci. 2015;237:33–45.

20. Hofmann K, Bucher P. The UBA domain: a sequence motif present in multiple enzyme classes of the ubiquitination pathway. Trends Biochem Sci. 1996;21(5):172–3.
21. Bhalerao RP, Salchert K, Bakó L, Okrész L, Szabados L, Muranaka T, Machida Y, Schell J, Koncz C. Regulatory interaction of PRL1 WD protein with Arabidopsis SNF1-like protein kinases. Proc Natl Acad Sci USA. 1999;96(9):5322–7.
22. Li R, Radani Y, Ahmad B, Movahedi A, Yang L. Identification and characteristics of SnRK genes and cold stress-induced expression profiles in Liriodendron chinense. BMC Genomics. 2022;23(1):708.
23. Monger WA, Thomas TH, Purcell PC, Halford NG. Identification of a sucrose nonfermenting-1-related protein kinase in sugar beet (Beta vulgaris L). Plant Growth Regul. 1997;22(3):181–8.
24. Kulik A, Wawer I, Krzywińska E, Bucholc M, Dobrowolska G. SnRK2 protein kinases–key regulators of plant response to abiotic stresses. Omics. 2011;15(12):859–72.
25. Ohta M, Guo Y, Halfter U, Zhu J-K. A novel domain in the protein kinase SOS2 mediates interaction with the protein phosphatase 2 C ABI2. Proc Natl Acad Sci USA. 2003;100(20):11771–6.
26. Albrecht V, Ritz O, Linder S, Harter K, Kudla J. The NAF domain defines a novel protein-protein interaction module conserved in Ca2+-regulated kinases. EMBO J. 2001;20(5):1051–63.
27. Jamsheer KM, Kumar M, Srivastava V. SNF1-related protein kinase 1: the many-faced signaling hub regulating developmental plasticity in plants. J Exp Bot. 2021;72(17):6042–65.
28. Son S, Im JH, Ko JH, Lee Y, Lee S, Han KH. SNF1-related protein kinase 1 represses Arabidopsis growth through post-translational modification of E2Fa in response to energy stress. New Phytol. 2023;237(3):823–39.
29. Wang K, Li M, Zhang B, Chang Y, An S, Zhao W. Sugar starvation activates the OsSnRK1a-OsbHLH111/OsSGI1-OsTPP7 module to mediate growth Inhibition of rice. Plant Biotechnol J. 2023;21(10):2033–46.
30. Lin CR, Lee KW, Chen CY, Hong YF, Chen JL, Lu CA, Chen KT, Ho TH, Yu SM. SnRK1A-interacting negative regulators modulate the nutrient starvation signaling sensor SnRK1 in source-sink communication in cereal seedlings under abiotic stress. Plant Cell. 2014;26(2):808–27.
31. Wang Y, Liu A. Genomic characterization and expression analysis of the SnRK family genes in Dendrobium officinale Kimura et Migo (Orchidaceae). Plants (Basel). 2021;10(3).
32. Mao X, Li Y, Rehman SU, Miao L, Zhang Y, Chen X, Yu C, Wang J, Li C, Jing R. The sucrose Non-Fermenting 1-Related protein kinase 2 (SnRK2) genes are multifaceted players in plant growth, development and response to environmental stimuli. Plant Cell Physiol. 2020;61(2):225–42.
33. Kawa D, Meyer AJ, Dekker HL, Abd-El-Haliem AM, Gevaert K, Van De Slijke E, Maszkowska J, Bucholc M, Dobrowolska G, De Jaeger G, et al. SnRK2 protein kinases and mRNA decapping machinery control root development and response to salt. Plant Physiol. 2020;182(1):361–77.
34. Wang X, Wang L, Wang Y, Liu H, Hu D, Zhang N, Zhang S, Cao H, Cao Q, Zhang Z, et al. Arabidopsis PCaP2 plays an important role in chilling tolerance and ABA response by activating CBF- and SnRK2-Mediated transcriptional regulatory network. Front Plant Sci. 2018;9:215.
35. Iglesias-Moya J, Benítez Á, Segura M, Alonso S, Garrido D, Martínez C, Jamilena M. Structural and functional characterization of genes PYL-PP2C-SnRK2s in the ABA signalling pathway of Cucurbita pepo. BMC Genomics. 2024;25(1):268.
36. Li J, Liu X, Ahmad N, Wang Y, Ge H, Wang Y, Liu W, Li X, Wang N, Wang F, et al. CePP2C19 confers tolerance to drought by regulating the ABA sensitivity in Cyperus esculentus. BMC Plant Biol. 2023;23(1):524.
37. Shao Z, Yang S, Gu Y, Guo Y, Zhou H, Yang Y. Ubiquitin negatively regulates ABA responses by inhibiting SnRK2.2 and SnRK2.3 kinase activity in Arabidopsis. J Exp Bot. 2023;74(17):5394–404.
38. Tajdel M, Mituła F, Ludwików A. Regulation of Arabidopsis MAPKKK18 by ABI1 and SnRK2, components of the ABA signaling pathway. Plant Signal Behav. 2016;11(4):e1139277.
39. Kolukisaoglu U, Weinl S, Blazevic D, Batistic O, Kudla J. Calcium sensors and their interacting protein kinases: genomics of the Arabidopsis and rice CBL-CIPK signaling networks. Plant Physiol. 2004;134(1):43–58.
40. Ma X, Li QH, Yu YN, Qiao YM, Haq SU, Gong ZH. The CBL-CIPK pathway in plant response to stress signals. Int J Mol Sci. 2020;21(16).
41. Kim KN, Lee JS, Han H, Choi SA, Go SJ, Yoon IS. Isolation and characterization of a novel rice Ca2+-regulated protein kinase gene involved in responses to diverse signals including cold, light, cytokinins, sugars and salts. Plant Mol Biol. 2003;52(6):1191–202.
42. Ai D, Wang Y, Wei Y, Zhang J, Meng J, Zhang Y. Comprehensive identification and expression analyses of the SnRK gene family in Casuarina equisetifolia in response to salt stress. BMC Plant Biol. 2022;22(1):572.
43. Liu J, Ishitani M, Halfter U, Kim CS, Zhu JK. The Arabidopsis thaliana SOS2 gene encodes a protein kinase that is required for salt tolerance. Proc Natl Acad Sci U S A. 2000;97(7):3730–4.
44. Wang G, Guan SL, Zhu N, Li Q, Chong X, Wang T, Xuan J. Comprehensive genomic analysis of SnRK in Rosaceae and expression analysis of RoSnRK2 in response to abiotic stress in Rubus occidentalis. Plants (Basel). 2023;12(9).
45. Zhang W, Hu H, Zhang S-B. Divergent adaptive strategies by two Co-occurring epiphytic orchids to water stress: escape or avoidance? Front Plant Sci. 2016;7:588.
46. Tay S, He J, Yam TW. CAM plasticity in epiphytic tropical Orchid species responding to environmental stress. Bot Stud. 2019;60(1):7.
47. Xie X, Lin M, Xiao G, Wang Q, Li Z. Identification and characterization of the AREB/ABF gene family in three Orchid species and functional analysis of DcaABI5 in Arabidopsis. Plants (Basel Switzerland). 2024;13(6).
48. Wang L, Zhao X, Zheng R, Huang Y, Zhang C, Zhang M-M, Lan S, Liu Z-J. Genome-Wide identification and drought stress response pattern of the NF-Y gene family in Cymbidium Sinense. Int J Mol Sci. 2024;25(5).
49. Zheng R, Chen J, Peng Y, Zhu X, Niu M, Chen X, Xie K, Huang R, Zhan S, Su Q, et al. General analysis of heat shock factors in the Cymbidium ensifolium genome provided insights into their evolution and special roles with response to temperature. Int J Mol Sci. 2024;25(2):1002.
50. Yang F, Gao J, Li J, Wei Y, Xie Q, Jin J, Lu C, Zhu W, Wong S-M, Zhu G. The China Orchid industry: past and future perspectives. Ornam Plant Res. 2024;4(1).
51. Hu Y, Liu J, Luo X, Cui R, Zhang L, Zhou L, Xu Z, Ma J. First report of Corynespora Cassiicola causing leaf spot on Jasminum nudiflorum in China. Plant Dis. 2023;107(8):2521.
52. Lai H, Wang M, Yan L, Feng C, Tian Y, Tian X, Peng D, Lan S, Zhang Y, Ai Y. Genome-Wide identification of bZIP transcription factors in Cymbidium ensifolium and analysis of their expression under Low-Temperature stress. Plants (Basel Switzerland). 2024;13(2).
53. Biswas SS, Pal R, De L, Kalaivanan N, Natta S, Alam BK, Ngangom N. A cultivation guide for Cymbidium growers. Indian Hortic. 2022;67:24–32.
54. Chen C, Wu Y, Li J, Wang X, Zeng Z, Xu J, Liu Y, Feng J, Chen H, He Y, et al. TBtools-II: A one for all, all for one bioinformatics platform for biological big-data mining. Mol Plant. 2023;16(11):1733–42.
55. Zhang D, Gao F, Jakovlić I, Zou H, Zhang J, Li WX, Wang GT. PhyloSuite: an integrated and scalable desktop platform for streamlined molecular sequence data management and evolutionary phylogenetics studies. Mol Ecol Resour. 2020;20(1):348–55.
56. Derelle R, Philippe H, Colbourne JK. Broccoli: combining phylogenetic and network analyses for orthology assignment. Mol Biol Evol. 2020;37(11):3389–96.
57. Zhang G, Hu Y, Huang M-Z, Huang W-C, Liu D-K, Zhang D, Hu H, Downing JL, Liu Z-J, Ma H. Comprehensive phylogenetic analyses of Orchidaceae using nuclear genes and evolutionary insights into epiphytism. J Integr Plant Biol. 2023;65(5):1204–25.
58. Miao B-B, Dong W, Gu Y-X, Han Z-F, Luo X, Ke C-H. You W-W: OmicsSuite: a customized and pipelined suite for analysis and visualization of multi-omics big data. Hortic Res. 2023;10(11):uhad195.
59. Wang Y, Tang H, Debarry JD, Tan X, Li J, Wang X, Lee T-h, Jin H, Marler B, Guo H, et al. MCScanX: a toolkit for detection and evolutionary analysis of gene synteny and collinearity. Nucleic Acids Res. 2012;40(7):e49.
60. Qiao X, Li Q, Yin H, Qi K, Li L, Wang R, Zhang S, Paterson AH. Gene duplication and evolution in recurring polyploidization-diploidization cycles in plants. Genome Biol. 2019;20(1):38.
61. Holub EB. The arms race is ancient history in arabidopsis, the wildflower. Nat Rev Genet. 2001;2(7):516–27.
62. Leister D. Tandem and segmental gene duplication and recombination in the evolution of plant disease resistance gene. Trends Genet. 2004;20(3):116–22.
63. Freeling M. Bias in plant gene content following different sorts of duplication: tandem, whole-genome, segmental, or by transposition. Annu Rev Plant Biol. 2009;60:433–53.
64. Marçais G, Delcher AL, Phillippy AM, Coston R, Salzberg SL, Zimin A. MUMmer4: A fast and versatile genome alignment system. PLoS Comput Biol. 2018;14(1):e1005944.
65. Dai X, Zhuang Z, Zhao PX. PsRNATarget: a plant small RNA target analysis server (2017 release). Nucleic Acids Res. 2018;46(W1):W49–54.
66. Shannon P, Markiel A, Ozier O, Baliga NS, Wang JT, Ramage D, Amin N, Schwikowski B, Ideker T. Cytoscape: a software environment for

integrated models of biomolecular interaction networks. Genome Res. 2003;13(11):2498–504.
67. Amin N, Du Y, Lu L, Khalifa MAS, Ahmad N, Ahmad S, Wang P. GmNAC3 acts as a key regulator in soybean against drought stress. Curr Plant Biology. 2024;38:100346.
68. Peršić V, Ament A, Antunović Dunić J, Drezner G, Cesar V. PEG-induced physiological drought for screening winter wheat genotypes sensitivity – integrated biochemical and chlorophyll a fluorescence analysis. Front Plant Sci. 2022;13:987702.
69. Agrawal L, Gupta S, Mishra SK, Pandey G, Kumar S, Chauhan PS, Chakrabarty D, Nautiyal CS. Elucidation of complex nature of PEG induced Drought-Stress response in rice root using comparative proteomics approach. Front Plant Sci. 2016;7:1466.
70. Song J, Henry H, Tian L. Drought-inducible changes in the histone modification H3K9ac are associated with drought-responsive gene expression in Brachypodium distachyon. Plant Biol. 2020;22(3):433–40.
71. Zhang Q, Ahmad N, Li Z, He J, Wang N, Naeem M, Jin L, Yao N, Liu X. CtCYP71A1 promotes drought stress tolerance and lignin accumulation in safflower and Arabidopsis. Environ Exp Bot. 2023;213:105430.
72. Hong Y, Ahmad N, Zhang J, Lv Y, Yao N. The CtMYB63 -CtU-box1-CtUCH1 module regulates cold tolerance and hydroxysafflor yellow A accumulation in Carthamus tinctorius. Ind Crops Prod. 2023;202:117088.
73. Ahmad N, Li T, Liu Y, Hoang NQV, Ma X, Zhang X, Liu J, Yao N, Liu X, Li H. Molecular and biochemical rhythms in dihydroflavonol 4-reductase- mediated regulation of Leucoanthocyanidin biosynthesis in Carthamus tinctorius L. Ind Crops Prod. 2020;156:112838.
74. Rehman A, Weng J, Li P, Shah IH, Rahman Su, Khalid M, Manzoor MA, Chang L, Niu Q. Green synthesized zinc oxide nanoparticles confer drought tolerance in Melon (Cucumis Melo L). Environ Exp Bot. 2023;212:105384.
75. Danquah A, de Zelicourt A, Colcombet J, Hirt H. The role of ABA and MAPK signaling pathways in plant abiotic stress responses. Biotechnol Adv. 2014;32(1):40–52.
76. Flavell RB. A framework for improving wheat Spike development and yield based on the master regulatory TOR and SnRK gene systems. J Exp Bot. 2023;74(3):755–68.
77. Wang Y, Yan H, Qiu Z, Hu B, Zeng B, Zhong C, Fan C. Comprehensive analysis of SnRK gene family and their responses to salt stress in Eucalyptus grandis. Int J Mol Sci. 2019;20(11):2786.
78. Kobayashi Y, Yamamoto S, Minami H, Kagaya Y, Hattori T. Differential activation of the rice sucrose nonfermenting1-related protein kinase2 family by hyperosmotic stress and abscisic acid. Plant Cell. 2004;16(5):1163–77.
79. Wang C, Abbas F, Zhou Y, Ke Y, Li X, Yue Y, Yu Y, Yu R, Fan Y. Genome-wide identification and expression pattern of SnRK gene family under several hormone treatments and its role in floral scent emission in Hedychium coronarium. PeerJ. 2021;9:e10883.
80. Zhang G-Q, Liu K-W, Li Z, Lohaus R, Hsiao Y-Y, Niu S-C, Wang J-Y, Lin Y-C, Xu Q, Chen L-J, et al. The apostasia genome and the evolution of orchids. Nature. 2017;549(7672):379–83.
81. Drerup MM, Schlücking K, Hashimoto K, Manishankar P, Steinhorst L, Kuchitsu K, Kudla J. The calcineurin B-like calcium sensors CBL1 and CBL9 together with their interacting protein kinase CIPK26 regulate the Arabidopsis NADPH oxidase RBOHF. Mol Plant. 2013;6(2):559–69.
82. Parenteau J, Maignon L, Berthoumieux M, Catala M, Gagnon V, Abou Elela S. Introns are mediators of cell response to starvation. Nature. 2019;565(7741):612–7.
83. Colina F, Amaral J, Carbó M, Pinto G, Soares A, Cañal MJ, Valledor L. Genome-wide identification and characterization of CKIN/SnRK gene family in Chlamydomonas reinhardtii. Sci Rep. 2019;9(1):350.
84. Ali GM, Komatsu S. Proteomic analysis of rice leaf sheath during drought stress. J Proteome Res. 2006;5(2):396–403.
85. Sarda X, Tousch D, Ferrare K, Legrand E, Dupuis JM, Casse-Delbart F, Lamaze T. Two TIP-like genes encoding Aquaporins are expressed in sunflower guard cells. Plant Journal: Cell Mol Biology. 1997;12(5):1103–11.
86. Zhao W, Cheng Y-H, Zhang C, Shen X-J, You Q-B, Guo W, Li X, Song X-J, Zhou X-A, Jiao Y-Q. Genome-Wide identification and characterization of the GmSnRK2 family in soybean. Int J Mol Sci. 2017;18(9).
87. Hussain Q, Asim M, Zhang R, Khan R, Farooq S, Wu J. Transcription factors interact with ABA through gene expression and signaling pathways to mitigate drought and salinity stress. Biomolecules. 2021;11(8).
88. Ritonga FN, Ngatia JN, Wang Y, Khoso MA, Farooq U, Chen S. AP2/ERF, an important cold stress-related transcription factor family in plants: A review. Physiol Mol Biology Plants: Int J Funct Plant Biology. 2021;27(9):1953–68.
89. Dahro B, Wang Y, Khan M, Zhang Y, Fang T, Ming R, Li C, Liu J-H. Two AT-Hook proteins regulate A/NINV7 expression to modulate sucrose catabolism for cold tolerance in Poncirus trifoliata. New Phytol. 2022;235(6):2331–49.
90. Islam W, Idrees A, Waheed A, Zeng F. Plant responses to drought stress: MicroRNAs in action. Environ Res. 2022;215(Pt 2):114282.
91. Sunkar R, Li Y-F, Jagadeeswaran G. Functions of MicroRNAs in plant stress responses. Trends Plant Sci. 2012;17(4):196–203.
92. Yan J, Zhao C, Zhou J, Yang Y, Wang P, Zhu X, Tang G, Bressan RA, Zhu J-K. The miR165/166 mediated regulatory module plays critical roles in ABA homeostasis and response in Arabidopsis thaliana. PLoS Genet. 2016;12(11):e1006416.
93. Yuan J, Wang X, Qu S, Shen T, Li M, Zhu L. The roles of miR156 in abiotic and biotic stresses in plants. Plant Physiol Biochemistry: PPB. 2023;204:108150.
94. Ma C, Burd S, Lers A. miR408 is involved in abiotic stress responses in Arabidopsis. Plant Journal: Cell Mol Biology. 2015;84(1):169–87.
95. Kumar RS, Sinha H, Datta T, Asif MH, Trivedi PK. microRNA408 and its encoded peptide regulate sulfur assimilation and arsenic stress response in Arabidopsis. Plant Physiol. 2023;192(2):837–56.
96. Ren Y-R, Zhao Q, Yang Y-Y, Zhang R, Wang X-F, Zhang T-E, You C-X, Huo H-Q, Hao Y-J. Interaction of BTB-TAZ protein MdBT2 and DELLA protein MdRGL3a regulates nitrate-mediated plant growth. Plant Physiol. 2021;186(1):750–66.
97. Wang Y-X, Yu T-F, Wang C-X, Wei J-T, Zhang S-X, Liu Y-W, Chen J, Zhou Y-B, Chen M, Ma Y-Z, et al. Heat shock protein TaHSP17.4, a TaHOP interactor in wheat, improves plant stress tolerance. Int J Biol Macromol. 2023;246:125694.
98. Mao J, Mo Z, Yuan G, Xiang H, Visser RGF, Bai Y, Liu H, Wang Q, van der Linden CG. The CBL-CIPK network is involved in the physiological crosstalk between plant growth and stress adaptation. Plant Cell Environ. 2023;46(10):3012–22.
99. Yoshida R, Umezawa T, Mizoguchi T, Takahashi S, Takahashi F, Shinozaki K. The regulatory domain of SRK2E/OST1/SnRK2.6 interacts with ABI1 and integrates abscisic acid (ABA) and osmotic stress signals controlling stomatal closure in Arabidopsis. J Biol Chem. 2006;281(8):5310–8.
100. Zhang WJ, Zhou Y, Zhang Y, Su YH, Xu T. Protein phosphorylation: A molecular switch in plant signaling. Cell Rep. 2023;42(7):112729.
101. Song J, Lin R, Tang M, Wang L, Fan P, Xia X, Yu J, Zhou Y. SlMPK1- and SlMPK2-mediated SlBBX17 phosphorylation positively regulates CBF-dependent cold tolerance in tomato. New Phytol. 2023;239(5):1887–902.
102. Wu XY, Li T. A casein kinase II phosphorylation site in AtYY1 affects its activity, stability, and function in the ABA response. Front Plant Sci. 2017;8:323.
103. Wang J, Sun Z, Chen C, Xu M. The MKK2a gene involved in the MAPK signaling cascades enhances Populus salt tolerance. Int J Mol Sci. 2022;23(17).
104. Halford NG, Hey SJ. Snf1-related protein kinases (SnRKs) act within an intricate network that links metabolic and stress signalling in plants. Biochem J. 2009;419(2):247–59.
105. Ramon M, Dang TVT, Broeckx T, Hulsmans S, Crepin N, Sheen J, Rolland F. Default activation and nuclear translocation of the plant cellular energy sensor SnRK1 regulate metabolic stress responses and development. Plant Cell. 2019;31(7):1614–32.
106. Lin Z, Li Y, Wang Y, Liu X, Ma L, Zhang Z, Mu C, Zhang Y, Peng L, Xie S, et al. Initiation and amplification of SnRK2 activation in abscisic acid signaling. Nat Commun. 2021;12(1):2456.
107. Chen Z, Zhou L, Jiang P, Lu R, Halford NG, Liu C. Genome-wide identification of sucrose nonfermenting-1-related protein kinase (SnRK) genes in barley and RNA-seq analyses of their expression in response to abscisic acid treatment. BMC Genomics. 2021;22(1):300.
108. Song J, Sun P, Kong W, Xie Z, Li C, Liu J-H. SnRK2.4-mediated phosphorylation of ABF2 regulates ARGININE DECARBOXYLASE expression and Putrescine accumulation under drought stress. New Phytol. 2023;238(1):216–36.
109. Lin Z, Li Y, Zhang Z, Liu X, Hsu C-C, Du Y, Sang T, Zhu C, Wang Y, Satheesh V, et al. A RAF-SnRK2 kinase cascade mediates early osmotic stress signaling in higher plants. Nat Commun. 2020;11(1):613.
110. Mishra S, Sharma P, Singh R, Tiwari R, Singh GP. Genome-wide identification and expression analysis of sucrose nonfermenting-1-related protein kinase (SnRK) genes in Triticum aestivum in response to abiotic stress. Sci Rep. 2021;11(1):22477.
111. Zhang Y, Ye Y, Jiang L, Lin Y, Gu X, Chen Q, Sun B, Zhang Y, Luo Y, Wang Y et al. Genome-Wide characterization of Snf1-Related protein kinases (SnRKs) and expression analysis of SnRK1.1 in strawberry. Genes. 2020;11(4).

Publisher's note